FR 09 , Kyoto, Japan
December 7-11, 2009
FR09P1277

Thermal and Hydrodynamic Fragmentation of a Single Molten Stainless Steel Droplet Penetrating Sodium Pool

Graduate School of Engineering
Hokkaido University
○ Ken-ichiro Sugiyama Zhi-gang Zhang

Objective

As a basic study to establish CORE CONCEPTs in metallic fuel SFRs with passive safety even in core disruptive accidents (CDAs), we have been carrying out a series of experiments on fragmentation of a single molten metal jet and droplet in small mass under a wide range of superheat and ambient Weber number(We_a) conditions.

In the today's presentation, we report the fragment data of a single molten droplet of stainless steel (304SS in the present study) used as the material constituting the reactor cores, to characterize the relationship between thermal effect and hydrodynamic effect in fragmentation of the molten core materials with interaction of sodium coolant.

Previous Experimental Studies

Gabor et al. conducted a series of experiments for fragmentation due to fuel-coolant interaction(FCI) between 3kg molten metallic fuel jet(mainly U-5mass%Zr, and U) and sodium coolant. Fragmentation suitable for quench was clearly observed in runs that even solid crust formation was observed because of spontaneous contact interface temperatures(T_i) well below their melting points.

However, the mechanism for fragmentation of molten metallic fuel jet with solid crust formation, which is important for safety, was not explained.

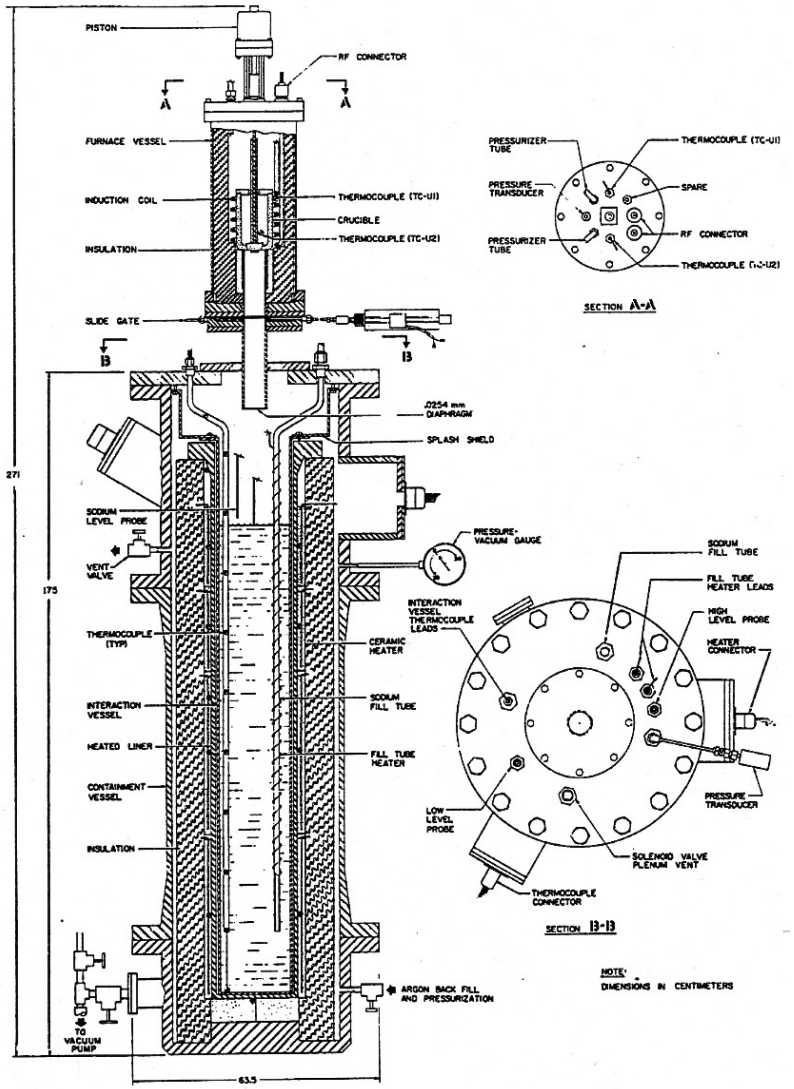

Fig. 1 Apparatus for Pour Stream Breakup

Table 1. Parameters for Pour Stream Breakup Experiments

Test	Melt Material	Melt[a] Superheat, °C	Sodium Temp, °C	Injection Velocity, m/s	Injection Diameter, mm	Melt Wt, kg	Sodium Depth, m	Comments
1	Sn	100	200	2	25	1.2	1.2	Proof test
2	U	100	600	2	25	3	1.2	Tests 2 and 3 study alloy effect
3	U-10Zr	100	600	2	25	3	1.2	
4	U-5Zr	100	600	2	25	3	1.2	Reference test
5	U-5Zr	10	600	2	25	3	1.2	Tests 5 and 6 study effect of melt superheat
6	U-5Zr	300	600	2	25	3	1.2	
7	U-5Zr	100	600	2	12.5	3	1.2	Injection dia. variation
8	U-5Zr	100	600	10	25	3	1.2	Injection vel. variation
9	U	400	600	2	25	3	0.9	Tests 9, 10, 11, and 12 study hydrodynamic breakup length and impingement heat flux
10	U	400	600	2	25	3	0.6	
11	U	400	600	2	25	3	0.3	
12	U	400	600	2	25	3	0.15	
13	U-10Fe	800	600	2	25	3	0.3	Tests 13 and 14 study behavior of low melting iron eutectic.
14	U-10Fe	800	600	2	25	3	0.9	

[a]Based on liquidus temperature of alloys.

Fig.1 Fragment Appearances of U-5mass%Zr Jet

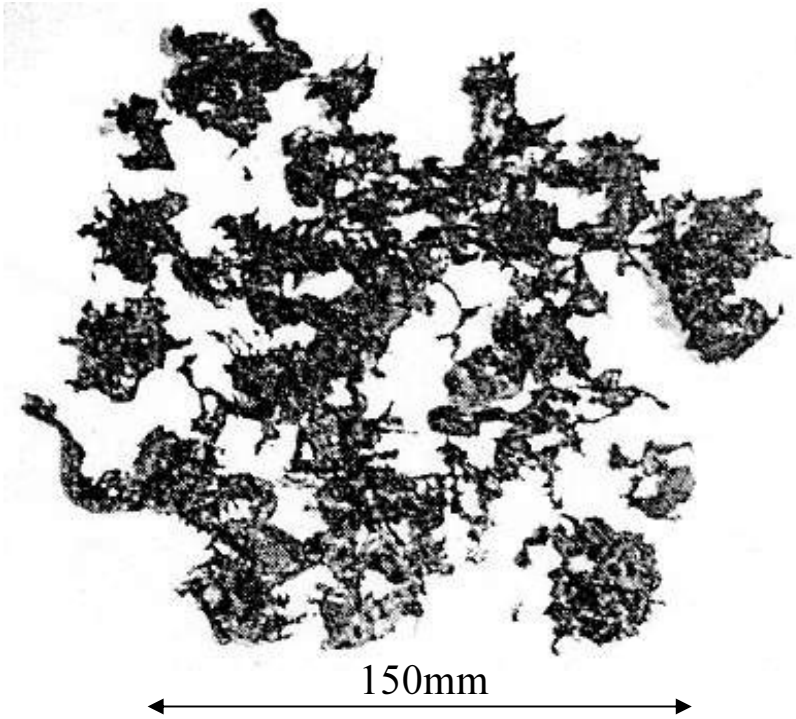

Large fragments at T_i of its melting point (No.6)

T_{sup}: 300℃, T_i : 1213℃, We_a : 52

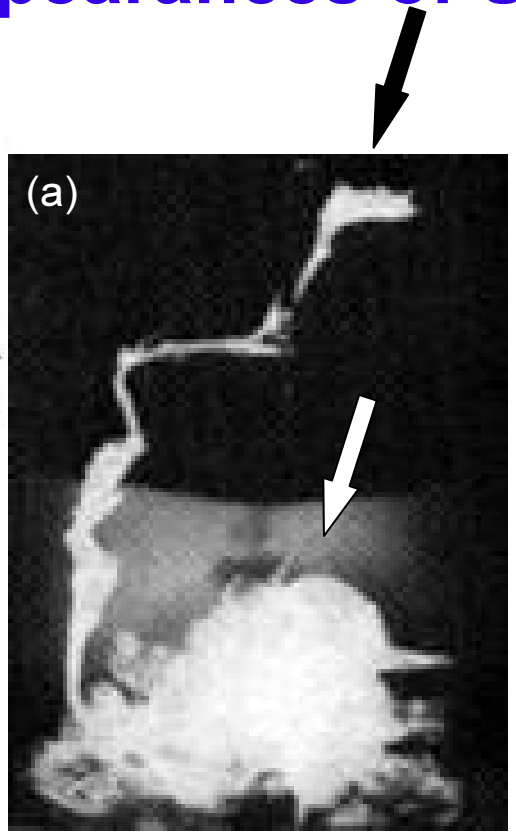

Radiograph of fragments at the bottom of the sodium pool

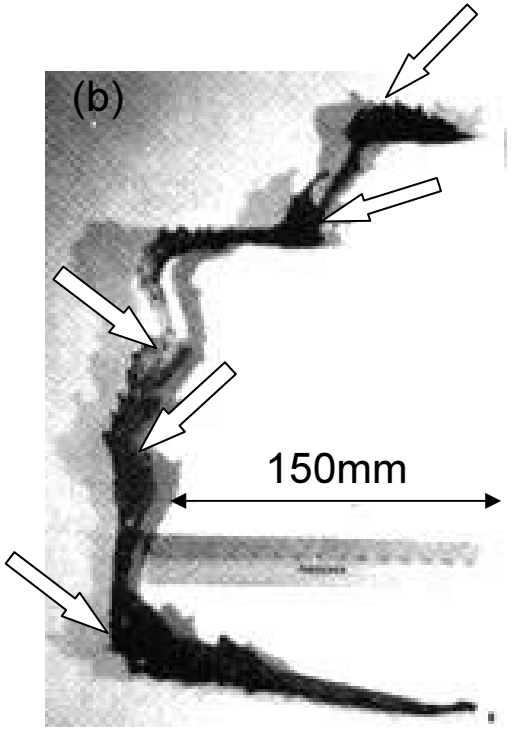

Frozen jet column with the large-scale structures

All fragments at T_i well below its melting point (No.5)

T_{sup}: 10℃, T_i :1094℃, We_a : 52

We Proposed Thermal Fragmentation Mechanism Combined with the Rapid Release of Latent Heat within a Single Molten Metal Jet with Solid Crust Formation.

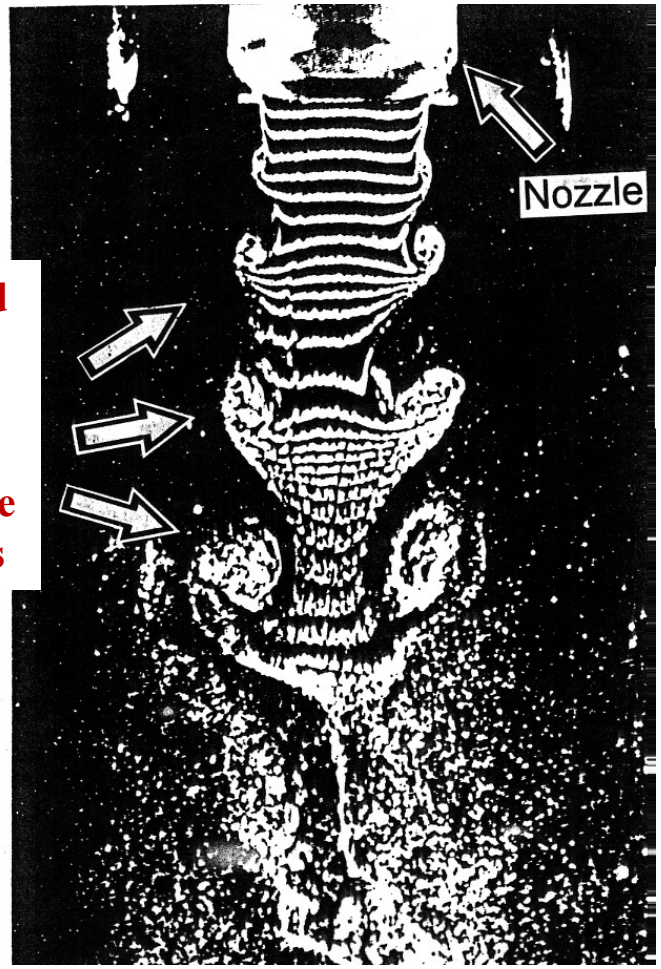

Organized motion makes the large- scale structures

Fig.2 Organized motion between water jet and the surrounding water

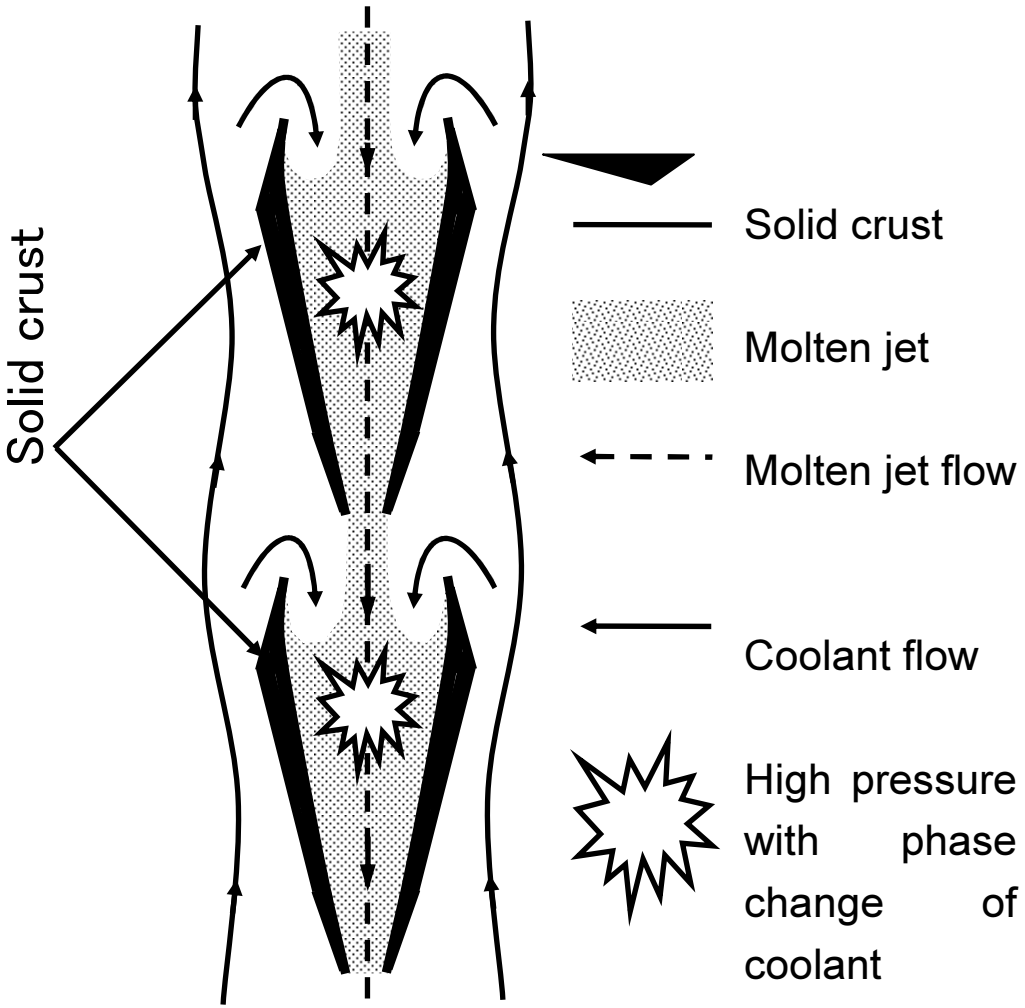

Fig.3 Sodium entrainment due to the organized motion between molten metal jet with solid crust and sodium coolant

We Also Reported Mass Median Diameters of Fragments Inversely Proportional to Latent Heat of Fusion for a Single Molten Metal Jet.

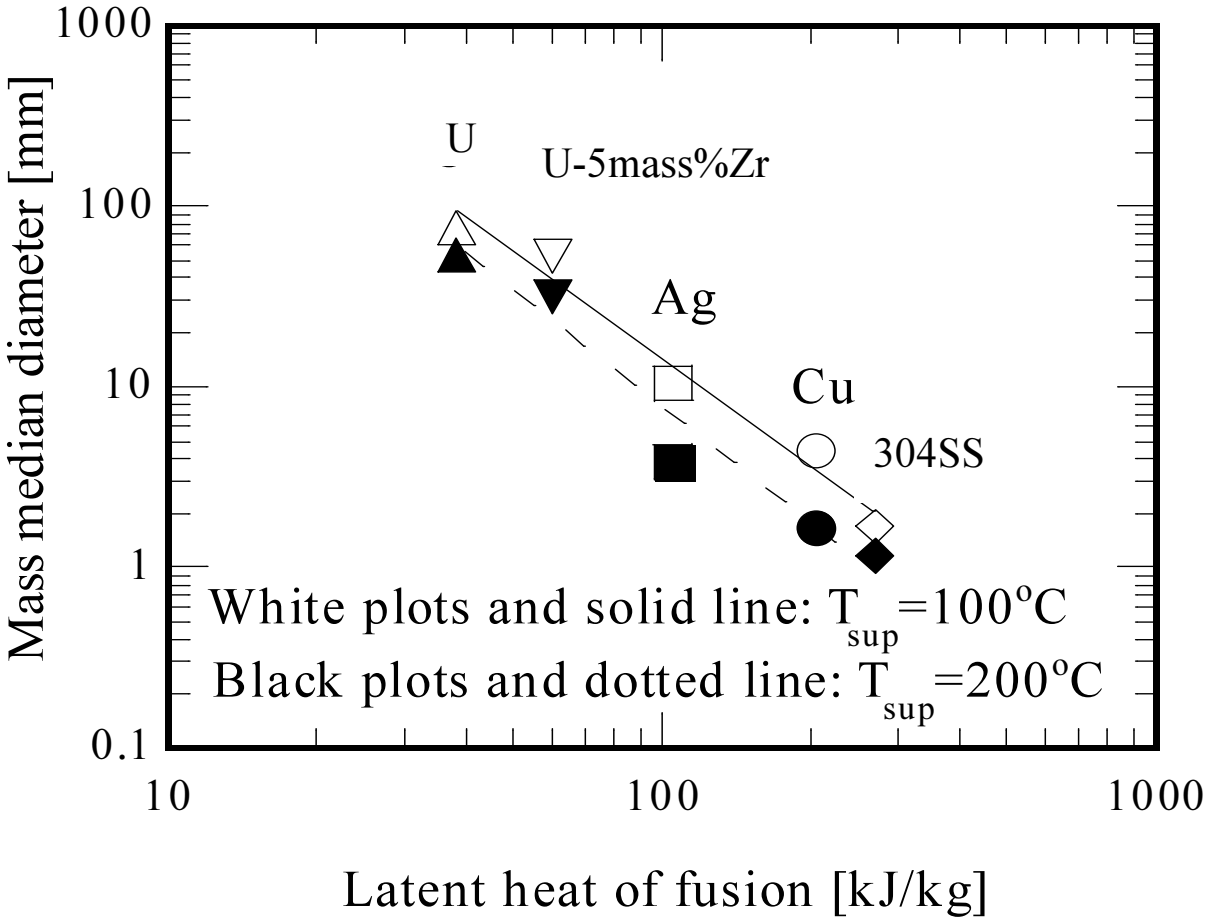

Fig.4 Latent heat of fusion vs. mass median diameter for molten metal and molten metallic fuel Jets

Present Experimental Apparatus and Conditions for 5g-304SS Droplet

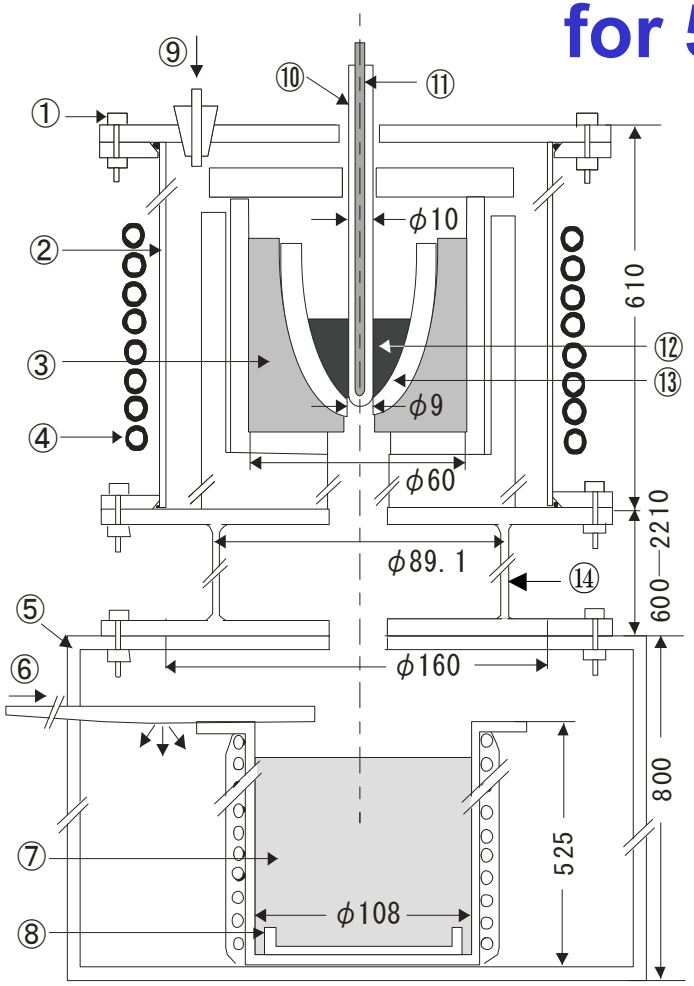

①Clamp bolt, ②Glass tube, ③Graphite crucible,④Induction coil, ⑤Polycarbonate box, ⑥⑨Ar gas, ⑦Sodium pot, ⑧ Catch pan, ⑩Alumina well,⑪Thermocouple, ⑫Stainless steel sample, ⑬Alumina pot, ⑭Extended tube

Fig. 5 Experimental apparatus

Table 2 Experimental conditions

Parameter		Sodium kept in pot	Cold trapped sodium
m_h	(g)	5g	5g
T_h	(℃)	1471～1703	1450～1699
T_c	(℃)	300～310	301～313
T_i	(℃)	903～1018	894～1018
We_a	(-)	226～586	199～305
Recovered mass (g)		2.95～4.77	2.98～4.37

Ambient Weber number (We_a)

A hydrodynamic parameter: the ratio of inertia force by falling velocity to surface tension.

$$We_a = \frac{\rho v^2}{\sigma / d}$$

where ρ is the density of the sodium, v is the velocity of the droplet, σ is the surface tension of the droplet, and d is the initial diameter of the droplet.

Result 1 : Fragment Size Distributions

304SS Droplet and jet with much difference in mass have little difference.

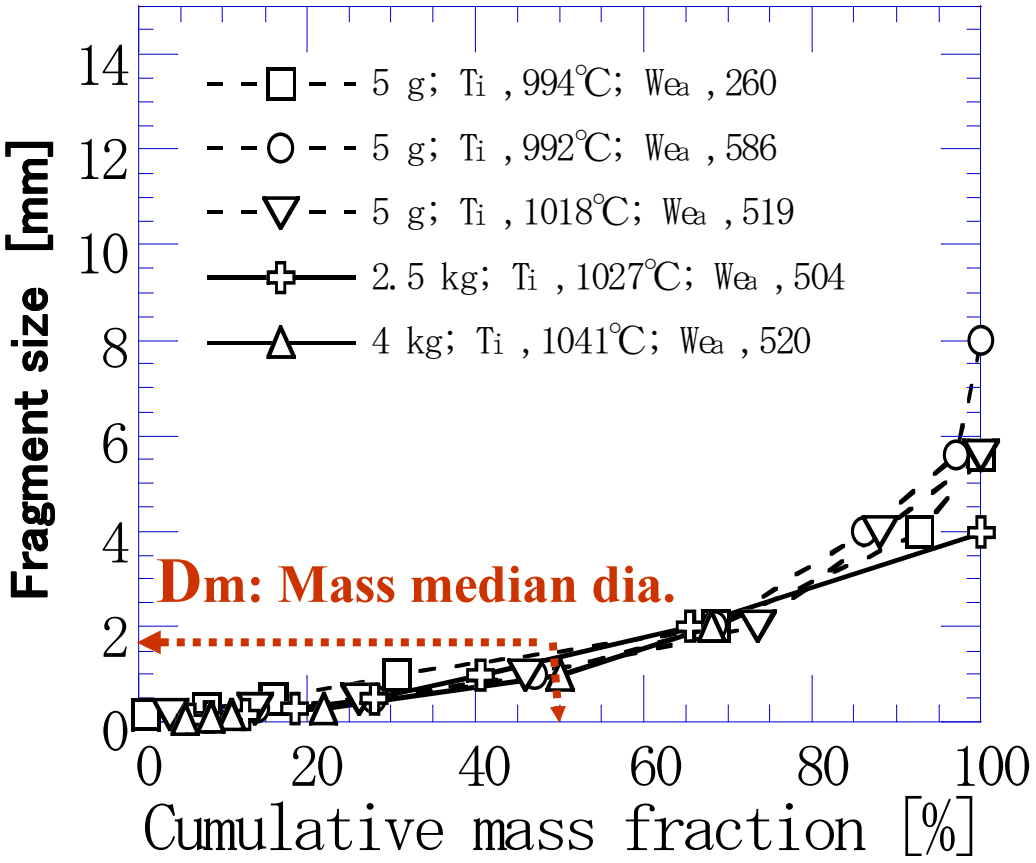

Fig. 6 Comparison of fragment size distributions for droplet and jet

Result 2 : Mass Median Dia.,D_m, Distributions

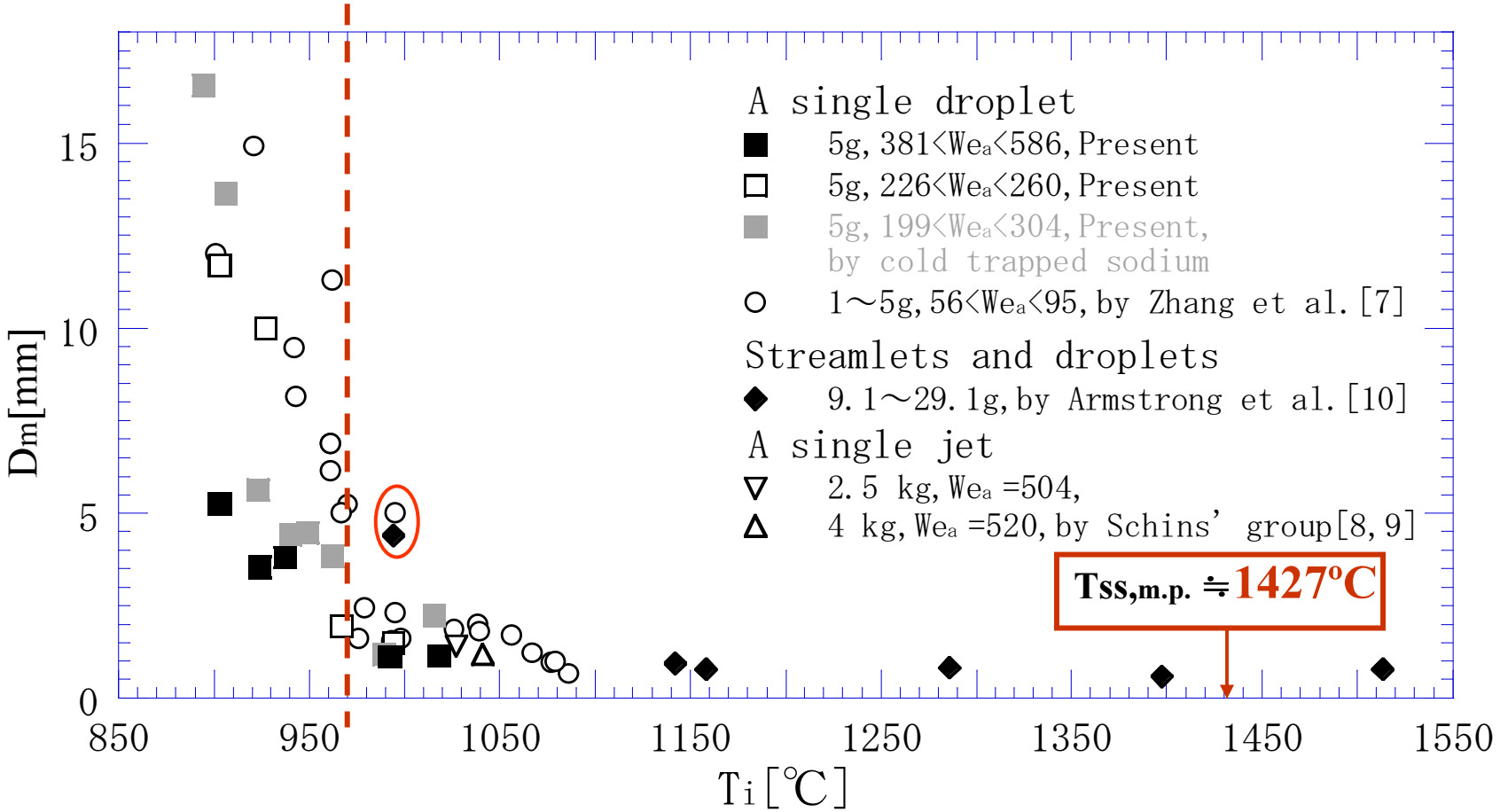

- Mass median diameter (D_m) : the size when the cumulative mass fraction is 50% of all the fragment mass.
- Instantaneous contact interface temperature (T_i) : the temperature is calculated as a one-dimensional heat conduction problem without the consideration of latent heat. → (Equation)

Fig. 7 D_m vs. T_i of droplet and jet fragments with different We_a

Fig.8 Fragment Appearances of 304SS Droplet at Low T_i with low Wea

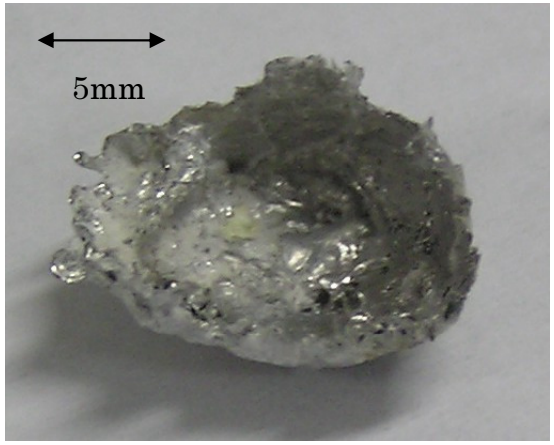

(a) Upper view of fragment a

(b) Bottom view of fragment a

(3 g; T_i, 970°C; We_a, 86)

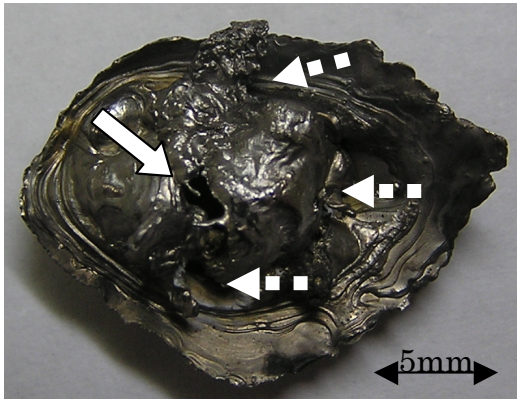

(a) Upper view of fragment b

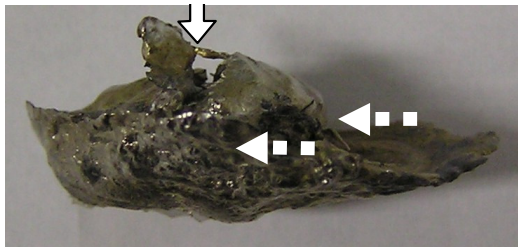

(b) Side view of fragment b

(5 g; T_i, 949°C; We_a, 81)

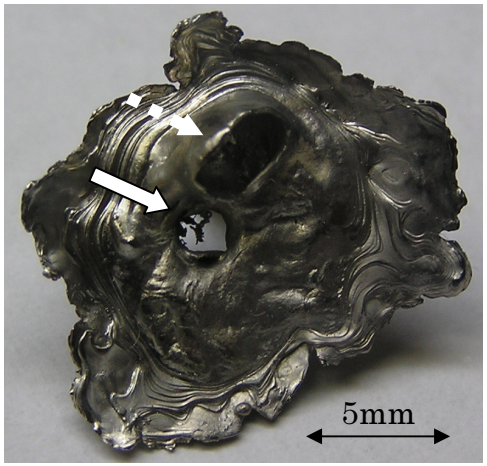

(a) Upper view of fragment c

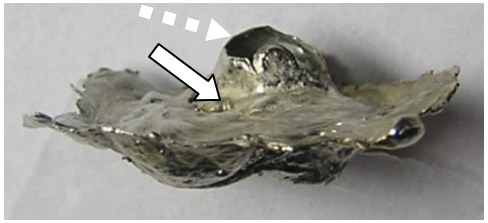

(b) Side view of fragment c

(5 g; T_i, 986 °C; We_a, 78)

Thermal Fragmentation mechanism of Droplet at Low T_i with low Wea

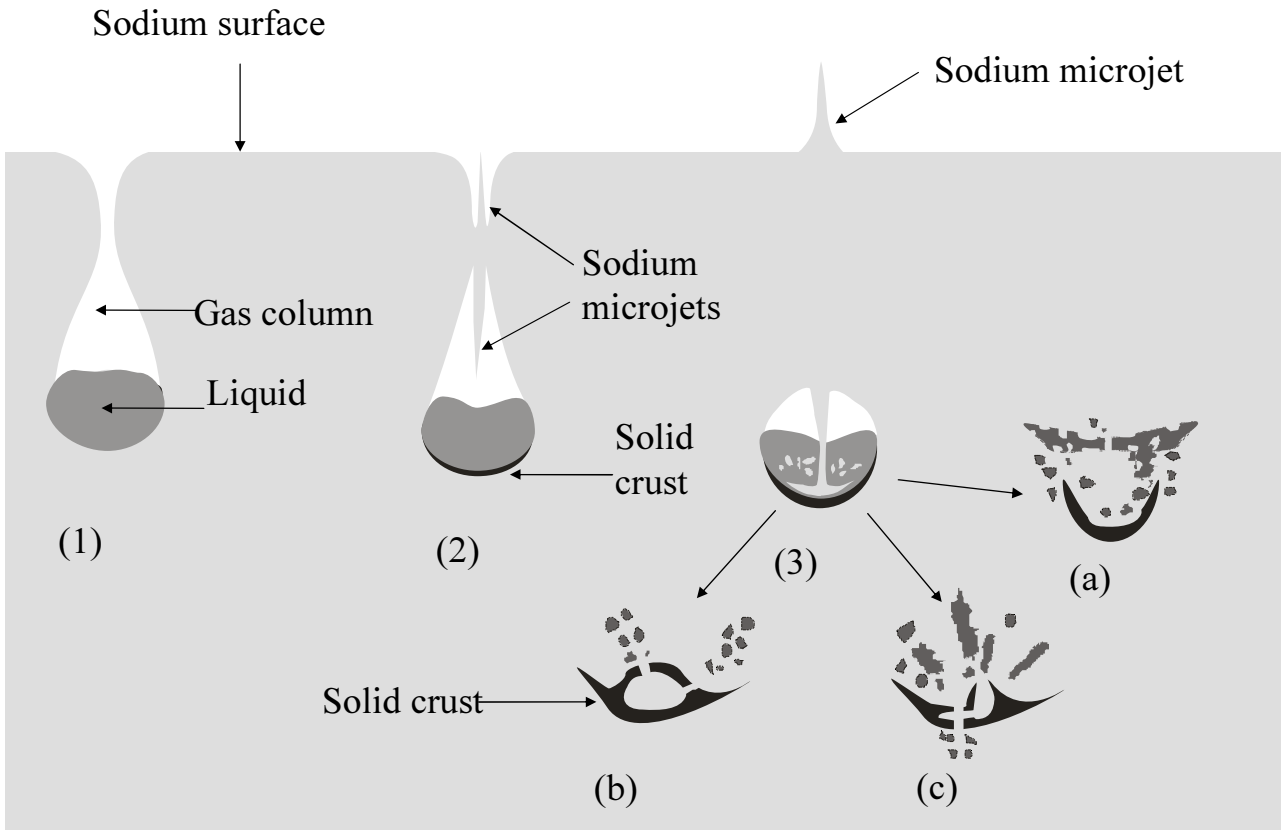

Figure 9 FCI image of molten droplet penetrating sodium

Result 3 : Normalized Dm/Do Distributions

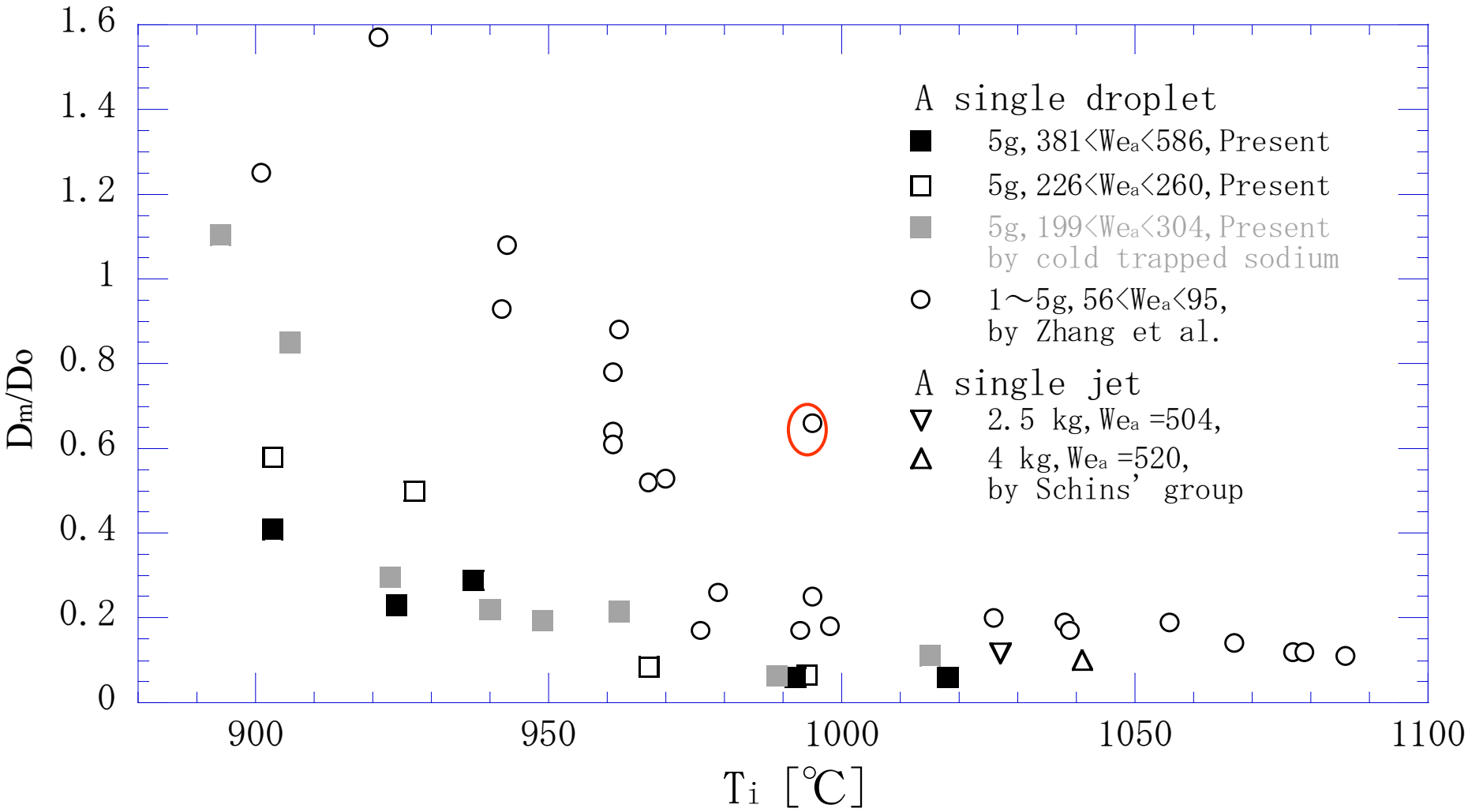

Fig. 10 Dm/Do vs. T_i of droplet and jet fragments

Result 4 : Comparison of Dm/Do Data Between SS Droplet, SS Jet and MF Jet

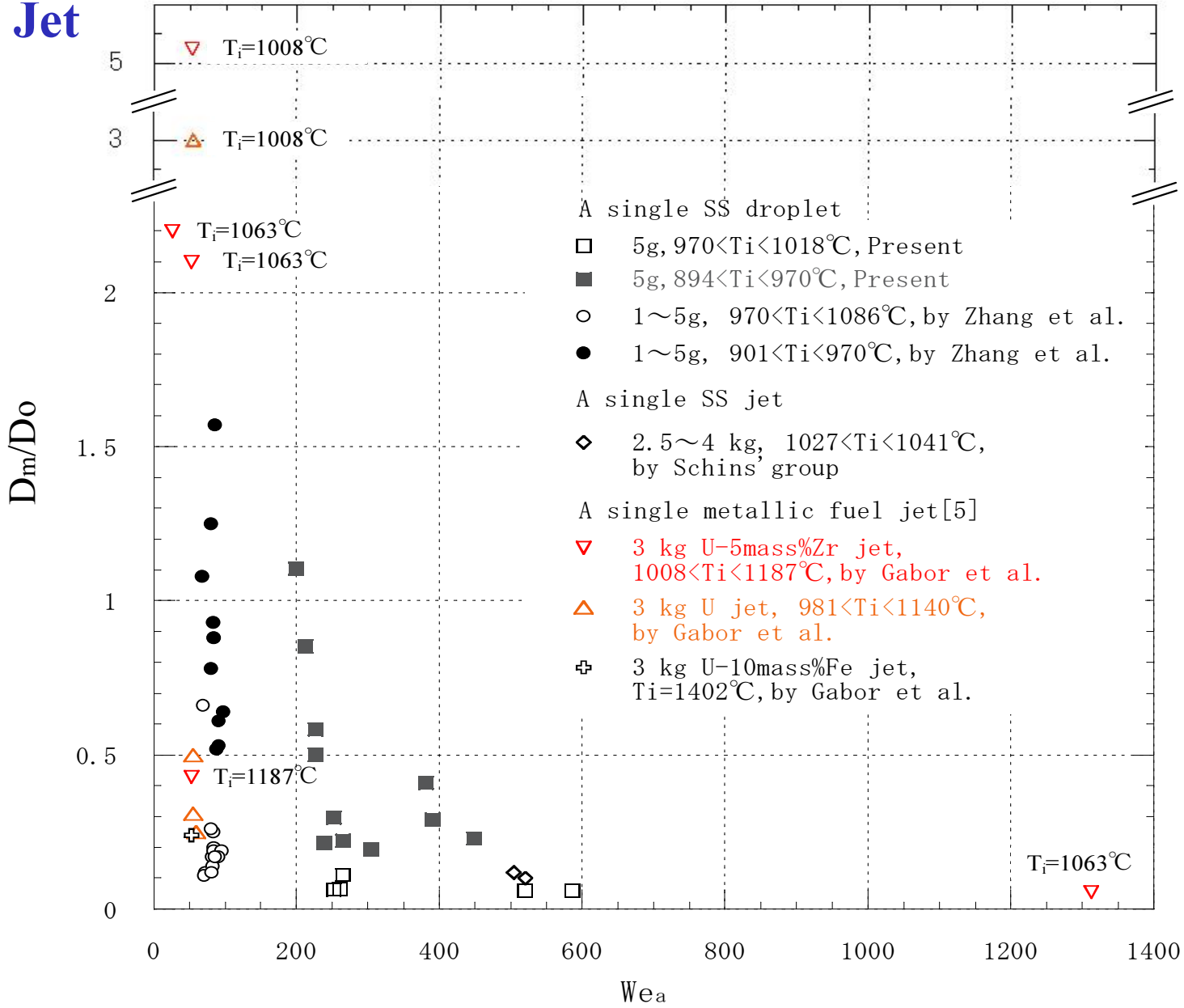

Fig. 11 Dm/Do vs. We_a of droplet and jet fragments with different T_i

Conclusions

1. The Dm values of a single molten stainless steel droplet with high T_i (Ti>970 ℃) , which characterize fragment size distributions, show low values suitable for quench even at T_i<<$T_{ss,mp}$. As We_a increases, the Dm values of a single molten stainless steel droplet with low T_i have a trend to converge low values suitable for quench even at T_i<<$T_{ss,mp}$ *because of* hydrodynamic effect in fragmentation.

2. The Dm values with high T_i (Ti>970℃) of a single molten stainless steel droplet, streamlets and droplets and jets even with 1000-fold difference in mass have almost the same level. Taking the difference of latent heat into consideration, there is possibility that the fragment sizes of molten core materials required for safety evaluation can be evaluated by simple molten metal experiments without enough consideration on modes and mass penetrating sodium pool.

Thanks for your attention !

A Configuration to Enhance Molten Fuel Discharge Proposed in JAEA

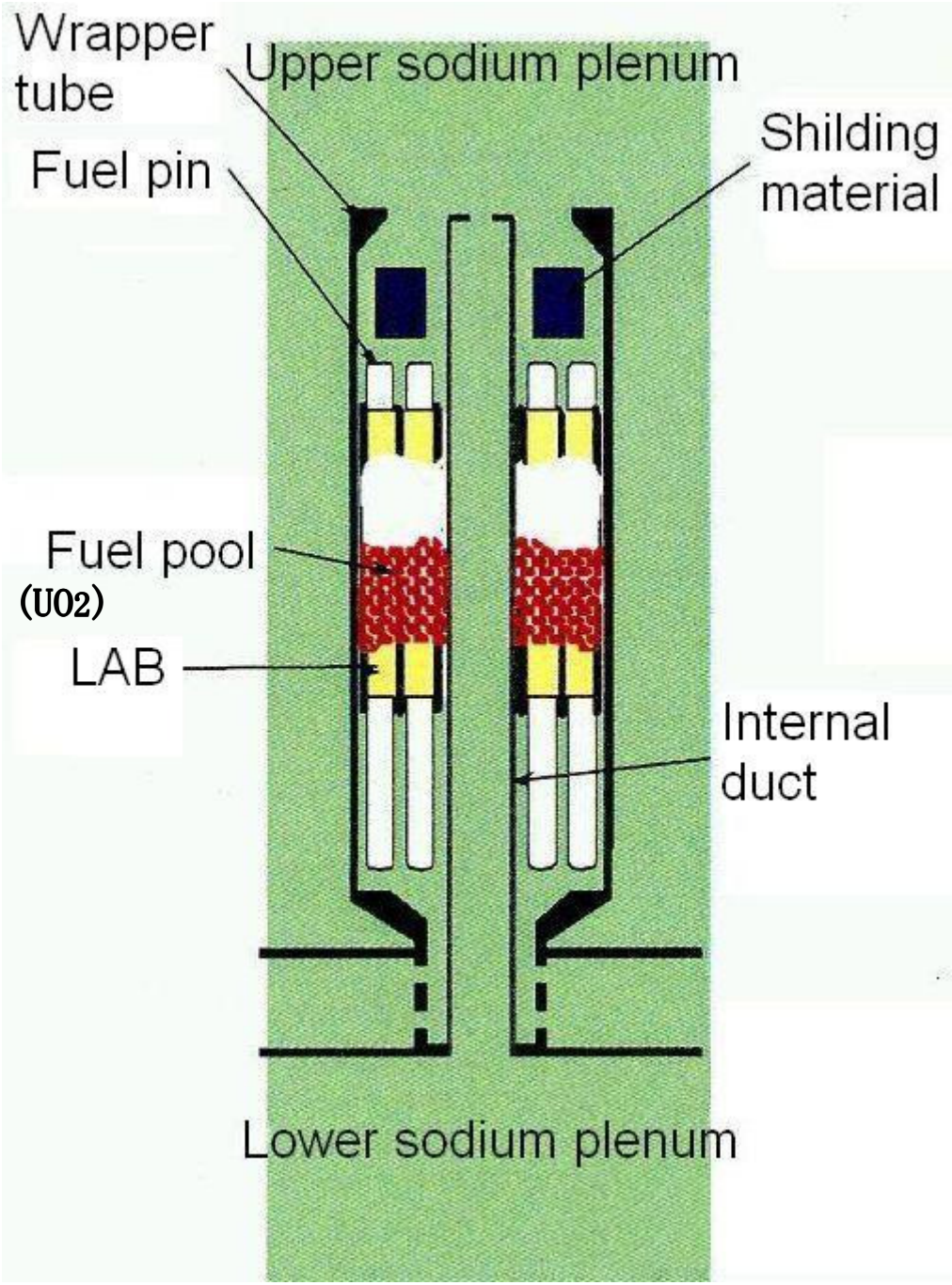

Table 3 T&P Properties of Strainless Steel, Copper, UO_2, Metallic Fuels, and Sodium

Thermophysical and physical property		Stainless steel[a]	Cu[a]	UO_2[b]	U[a]	U-15Pu-10Zr[a]	U-5Zr[a]	Na[g]
Melting point	[℃]	1427	1083	2865	1133	1156[c]	1214[c]	98
Boiling point	[℃]	2817	2587	3530	4400	—	—	881
Density	[kg/m^3]	6920	7919	8660	17797	14927[d]	16348[d]	892
Specific heat	[kJ/kg/K]	0.775	0.495	0.50[e]	0.160[f]	0.205[d]	0.185[d]	1.320
Heat capacity	[$kJ/m^3/K$]	5363	3920	4330	2848	3060	3024	1177
Thermal conductivity	[W/m/K]	18.3	169.5	8.4	42.3[f]	33.6[d]	39.9[d]	79.5
Thermal diffusivity	[mm^2/s]	3.41	43.30	2.20	14.90	11.00[d]	13.2[d]	65.60
Latent heat	[kJ/kg]	270.0	205.0	277.0	38.2	83.2[d]	60[d]	115.0
Kinetic viscosity	[mm^2/s]	0.775	0.477	0.480	0.309	0.377[d]	0.355[d]	0.456
Surface tension	[mN/m]	1830[d]	1272	450	1550	1390[d]	1540[d]	182

[a]Values at T_{sup} =100 ℃.

[b]Values at 3000 ℃.

[c]Solidus temperature.

[d]Values obtained by interpolation of mole fraction among two or three elements.

[e]Liquidus temperature.

[f]Values in solid state.

[g]Values at 250 ℃.

Background

In metallic fuel LMFRs, the occurrence of core disruptive accidents (CDAs) has been considered due to their neutron kinetics (positive void coefficient in large core) different from light water reactors.

Although the probability of occurrence of CDAs is quite low because of active and passive shutdown systems, it is indispensable for predicting the event sequence of damaged cores for the evaluation of potential risk of CDAs.

The major initiators of CDAs are anticipated transients without scram (ATWS). Typical ATWS events are unprotected transient overpower and unprotected loss of flow.

Background (cont'd)

The molten metallic fuel and structural material discharge from a core region due to the molten core materials – sodium coolant interaction is an important factor to consider the progression of CDAs in metallic fuel LMFRs.

If an appropriate quantity of molten core materials ejected in subassemblies is discharged from the core region and is finely fragmented for cooling, CDAs will terminate due to the insertion of sufficient negative reactivity to the core.

On the other hand, if molten core materials ejected in subassemblies at their near freezing points are solidified in the core region or in the lower plenum without fragmentation, the coolability of the core will deteriorate and the risk of re–criticality may arise, resulting in a more critical scenario.

Previous Experimental Study (2)

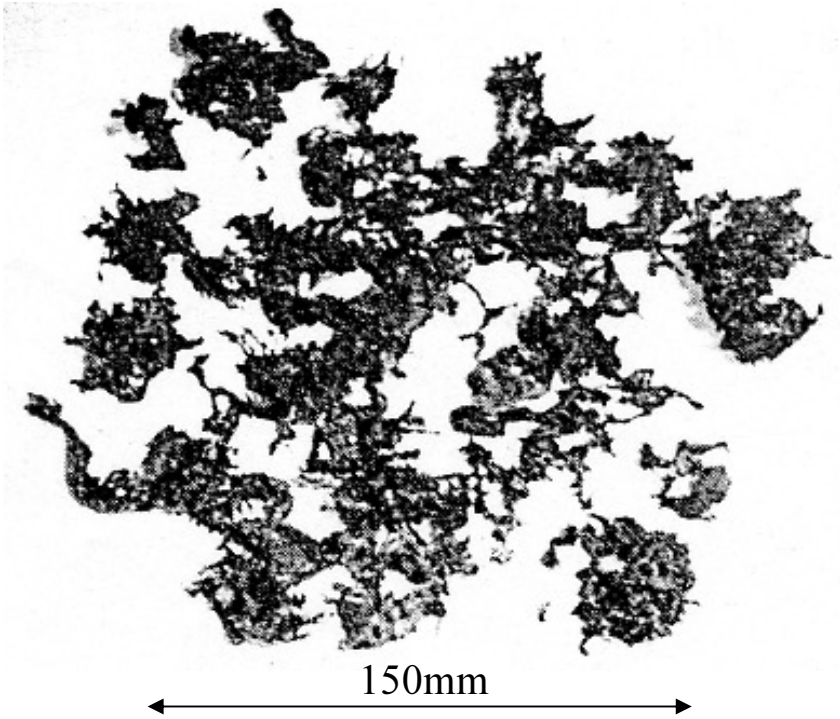

Large fragments observed in Test 6

T_h : 1551℃ / 3kg, T_{sup}: 300℃,
T_i : 1213℃, We_a : 52

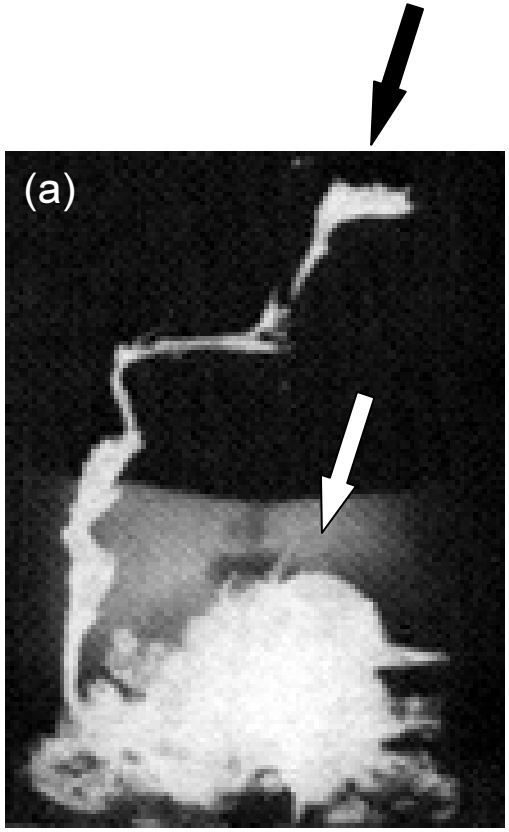

Radiograph of fragments at the bottom of the sodium pool

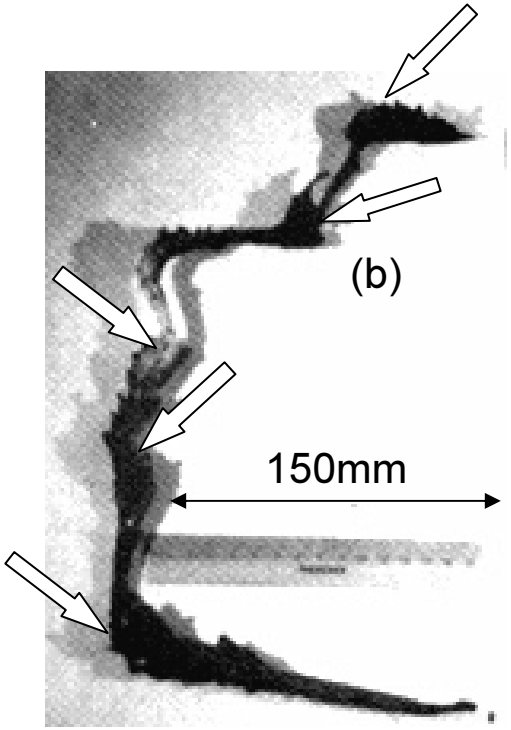

Frozen jet column with the large-scale structure

T_h :1261℃ / 3kg, T_{sup}: 10℃,
T_i :1094℃, We_a : 52

Typical appearance of U-5wt%Zr alloy fragments

Mass Median Dia. in Different Metals Including Our Data

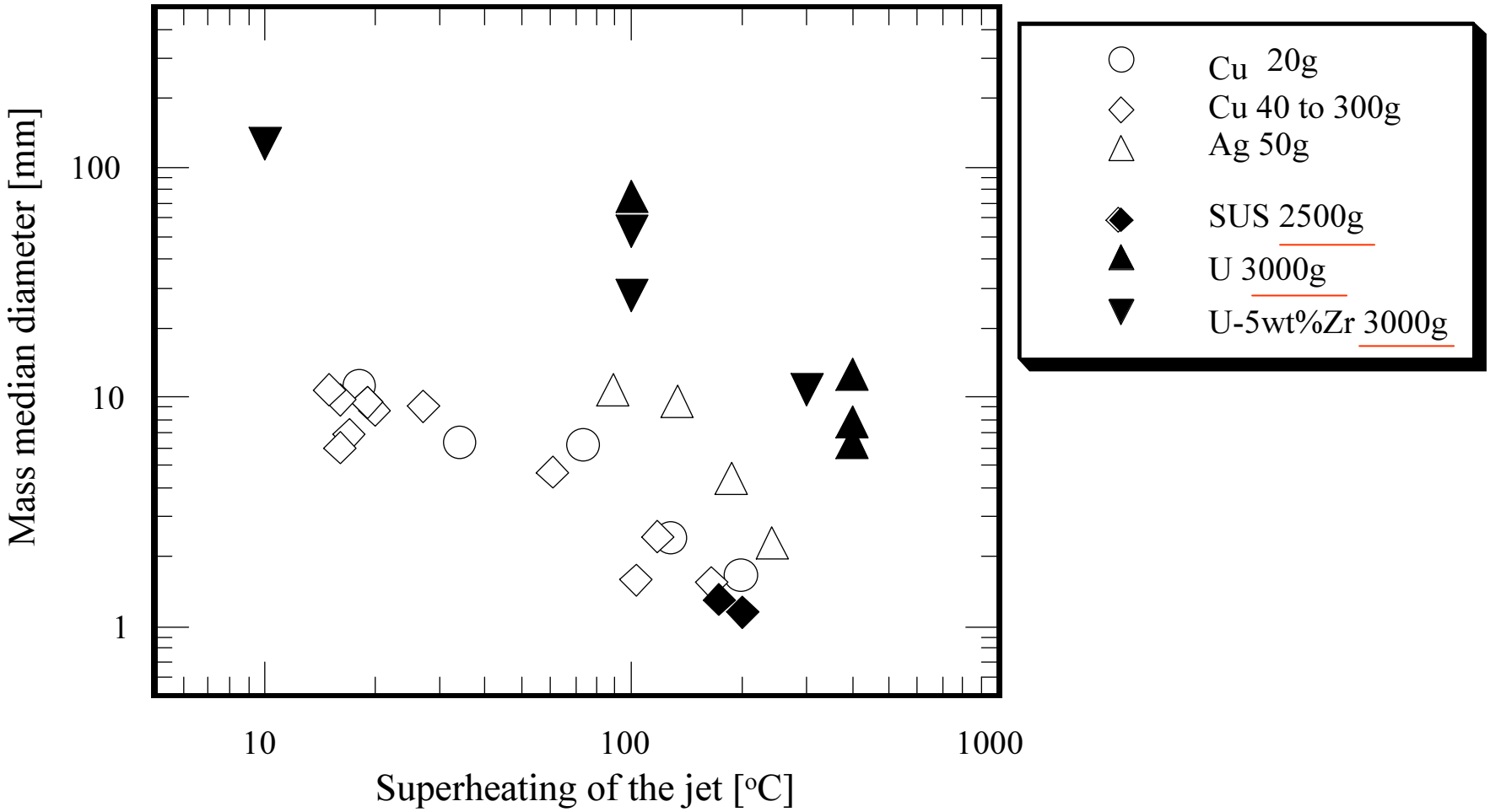

Mass median diameter vs. superheating under condition of solid crust formation

Previous Experimental Study (4)

Fragmentation of a Single Molten Metal Droplet Penetrating a Sodium Pool - II Stainless Steel and the Relationship with Copper Data-,

Z.G. Zhang and K.Sugiyama, Published in J. Nucl. Sci. Technol (2010).

Our group conducted an experiment of a single molten 304SS droplet (1-5g) penetrating a sodium pool at the instantaneous contact interface temperatures below its melting point with low ambient Weber number from 56 to 95, and confirmed that the fragmentation mechanism of entrapment type compared with results of copper droplet.

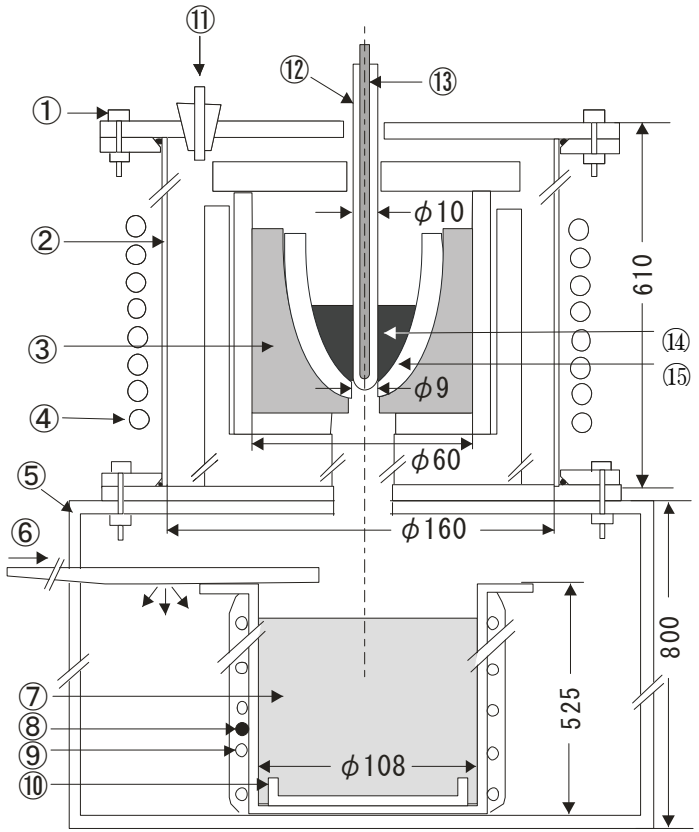

Apparatus for stainless steel droplet Breakup

Setup of Experimental Apparatus

Dropping height :
1.20-2.81m

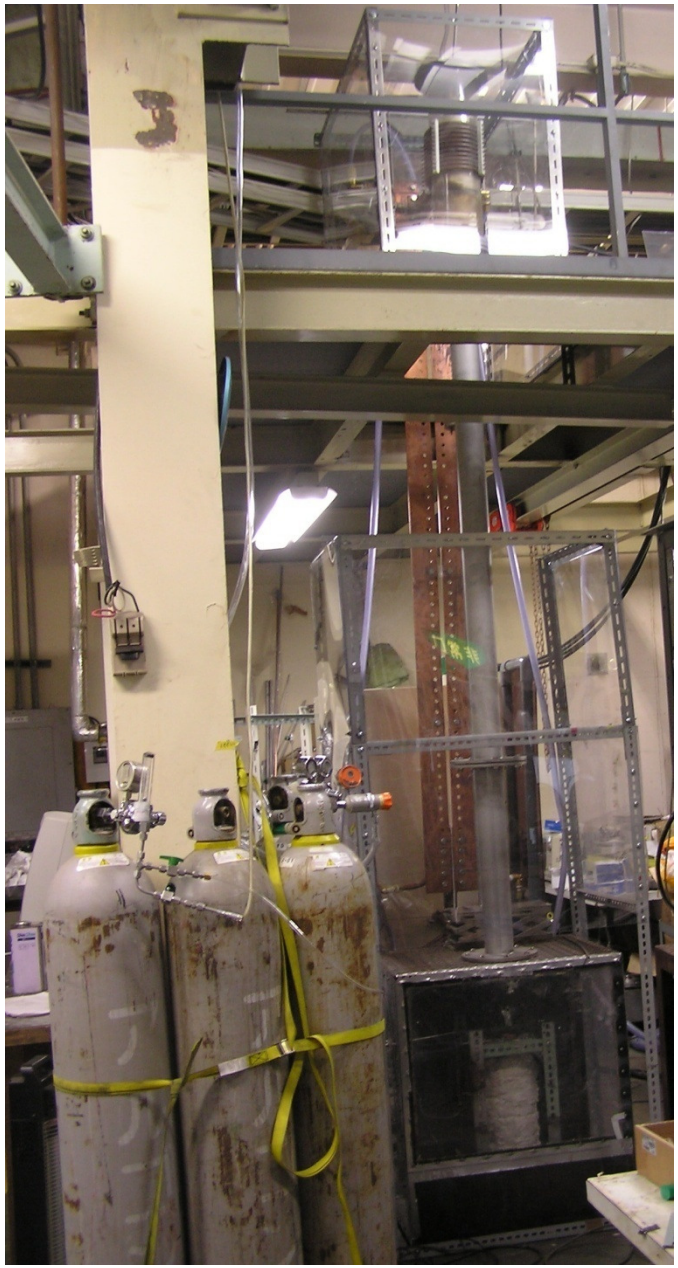

Fig.2
Practical experimental apparatus

Previous Experimental Study (3)

1) Boiling and fragmentation behaviour during fuel-sodium interactions,
by H. Schins, F. S. Gunnerson, Published in Nucl. Eng. Des., (1986).
2) Boiling fragmentation of molten stainless steel and copper in sodium,
by R. Benz, H. Schins, Published in Nucl. Eng. Des., (1982).

Schins'group reported the fine fragmentation experiment in which about 2.5 and 4 kg molten stainless steel jets were released into a sodium pool of 400℃ through a 12 mm nozzle in diameter with high Wea.

However, the two jet data were not enough.

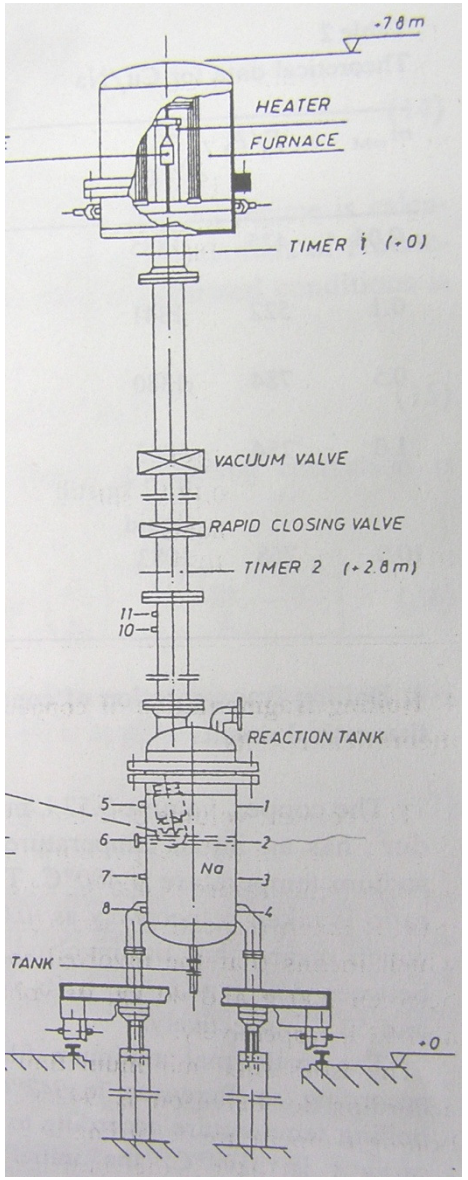

Apparatus for Jet Breakup

Previous Experimental Study (2)

Interaction of sodium with molten UO_2 and stainless steel using a dropping mode of contact,

by D.R.Armstrong et al., Reported in Reactor Technology, ANL-7890 (1971).

Armstrong et al. reported the fine interaction fragmentation by using the molten stainless steel (304SS streamlets and droplets) penetrating liquid sodium under the high superheat temperature condition, 6 data were provided without detailed hydrodynamic parameters.

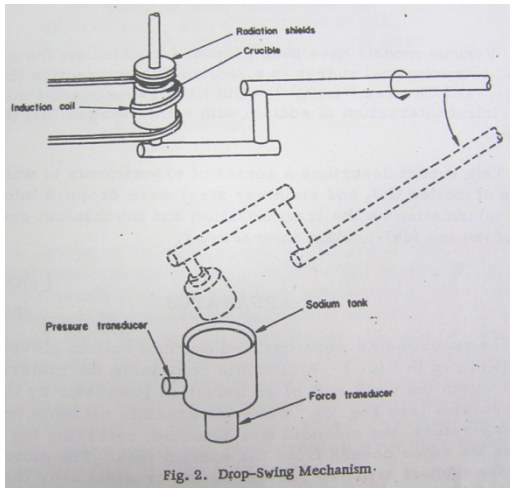

Droplet-Swing Apparatus

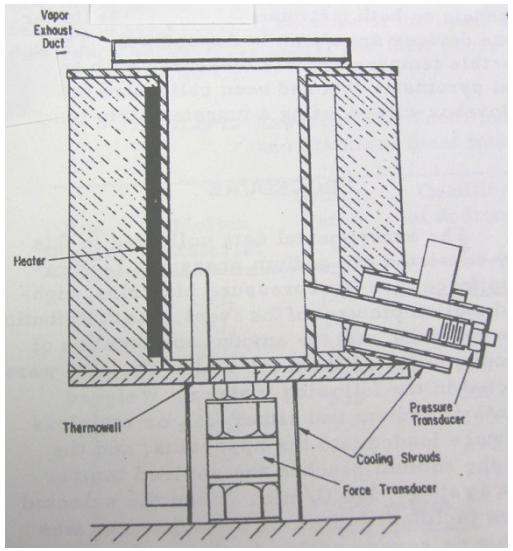

Sodium Tank Assembly

Selection of Simulant Material

Table 1 T&P Properties of Structural material, Metallic Fuels, and Sodium

Thermophysical and physical property		Stainless steel[a]	U[a]	U-5Zr[a]	Na[b]
Melting point	[℃]	1427	1133	1214[c]	98
Boiling point	[℃]	2817	4400	—	881
Density	[kg/m^3]	6920	17797	16348[d]	892
Specific heat	[kJ/kg/K]	0.775	0.160[e]	0.185[d]	1.320
Heat capacity	[kJ/m^3/K]	5363	2848	3024	1177
Thermal conductivity	[W/m/K]	18.3	42.3[e]	39.9[d]	79.5
Thermal diffusivity	[mm^2/s]	3.41	14.90	13.2[d]	65.60
Latent heat	[kJ/kg]	270.0	38.2	60[d]	115.0
Kinetic viscosity	[mm^2/s]	0.775	0.309	0.355[d]	0.456
Surface tension	[mN/m]	1830[d]	1550	1540[d]	182

[a]Values at T_{sup} =100 ℃. [b]Values at 250 ℃. [c]Solidus temperature.

[d]Values obtained by interpolation of mole fraction among two or three elements. [e]Values in solid state.

Previous Experimental Study (2)

Thermal interaction in crusted melt jets with large-scale structures

by K. Sugiyama, F. Sotome, and M. Ishikawa,
Published in Nuclear Engineering and Design, 189, pp. 329-336 , 1999.

The FCI between a jet of molten tin or zinc (100g) and water at T_is below its melting point is studied, a thermal fragmentation mechanism of entrainment type originating in the inside of jet is proposed based on the shapes of jet fragments as the large-scale structures produced by the organized motion.

Fragmentation mechanism of a single molten-copper drop falling in sodium pool with its melting point

by K.Sugiyama, et al.,
Published in J. Nucl. Sci. Technol., 42[12], 83-86,2000 .

The FCI experiment between a single molten copper droplet and sodium was conducted to confirm the same kind of fragmentation caused by the rapid release of latent heat even at the lowest T_i obtained at the melting point of copper, which means no superheating and supercooling. A thermal fragmentation mechanism of entrapment type on a single droplet is again proposed.

Previous Experimental Study (4)

Thermal interaction between molten metal jet and sodium pool: effect of principal factors governing fragmentation of the jet

by Nishimura, et al.,
Published in J.Nucl.Sci.Technol.103[3], 2010.

Nishimura *et al.* confirmed the the effect of hydrodynamic fragmentation with the high ambient Weber number (We_a > 200) becomes predominant over that of thermal fragmentation under the low superheat condition (T_{sup} < 165℃) by conducting experiments of molten copper jets (20－300 g) with We_a from 5 to 1,534 penetrating a sodium pool with the comparison of the molten metallic fuels from Gabor *et al.*.

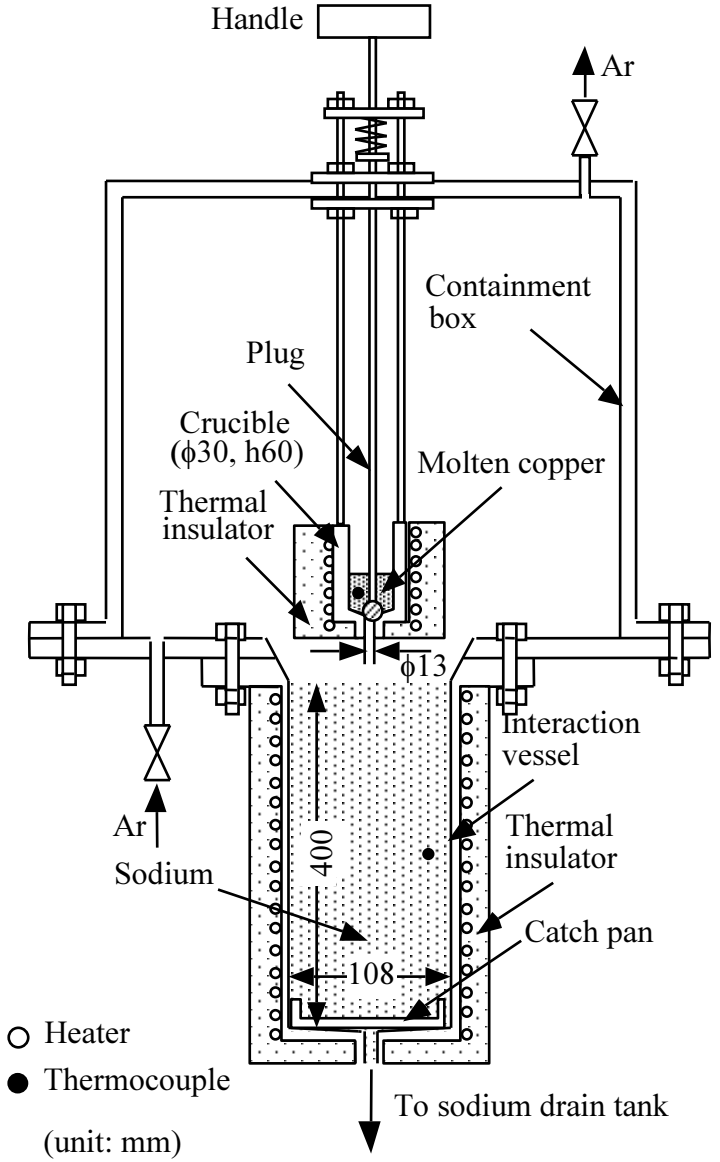

Apparatus for Jet Breakup

Result 4 : All Dm/Do Distributions

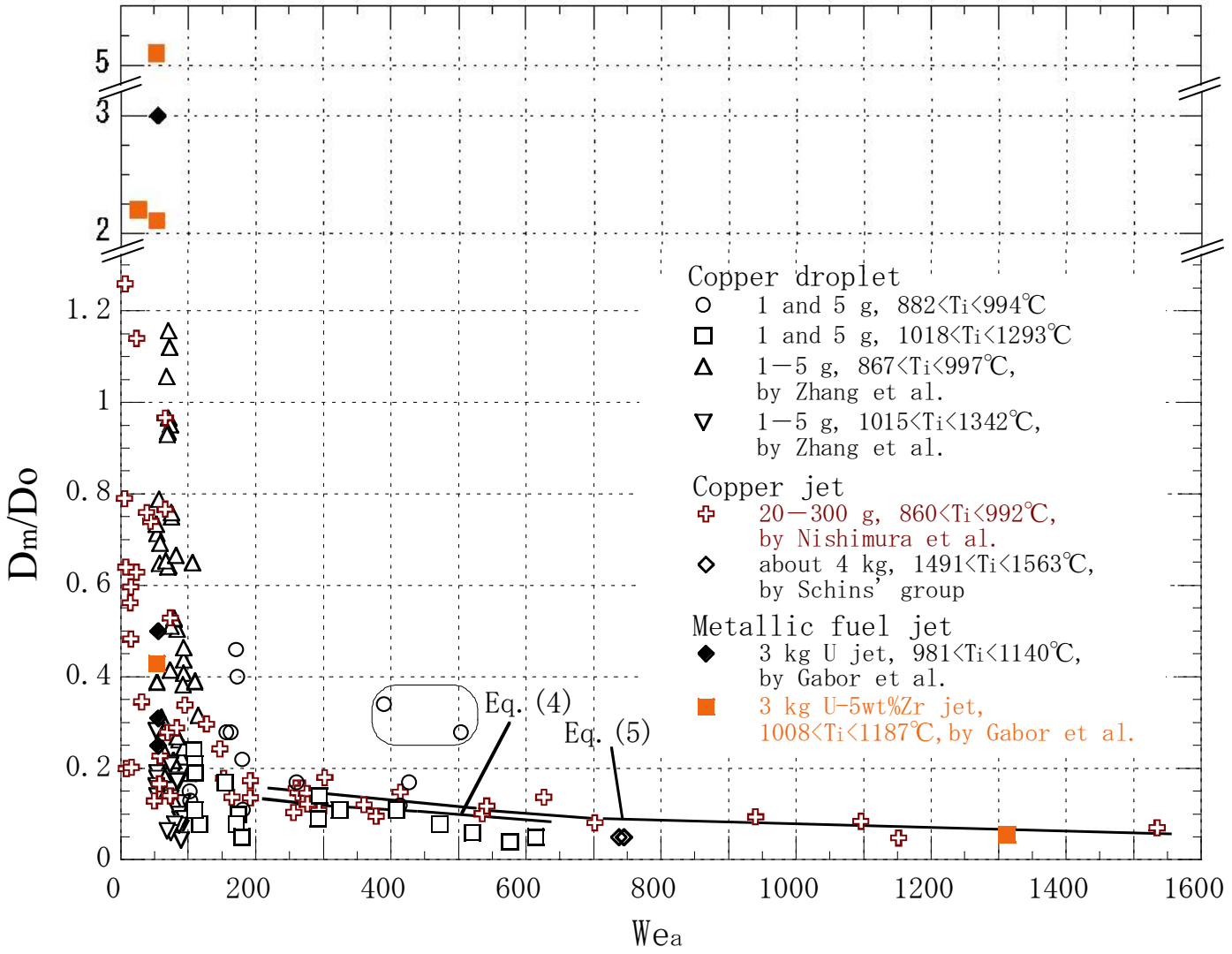

Fig. 6 Dm/Do versus We_a of copper droplet and jet and metallic fuel jet fragments

Result 4 : Dm/Do versus Wea Distributions

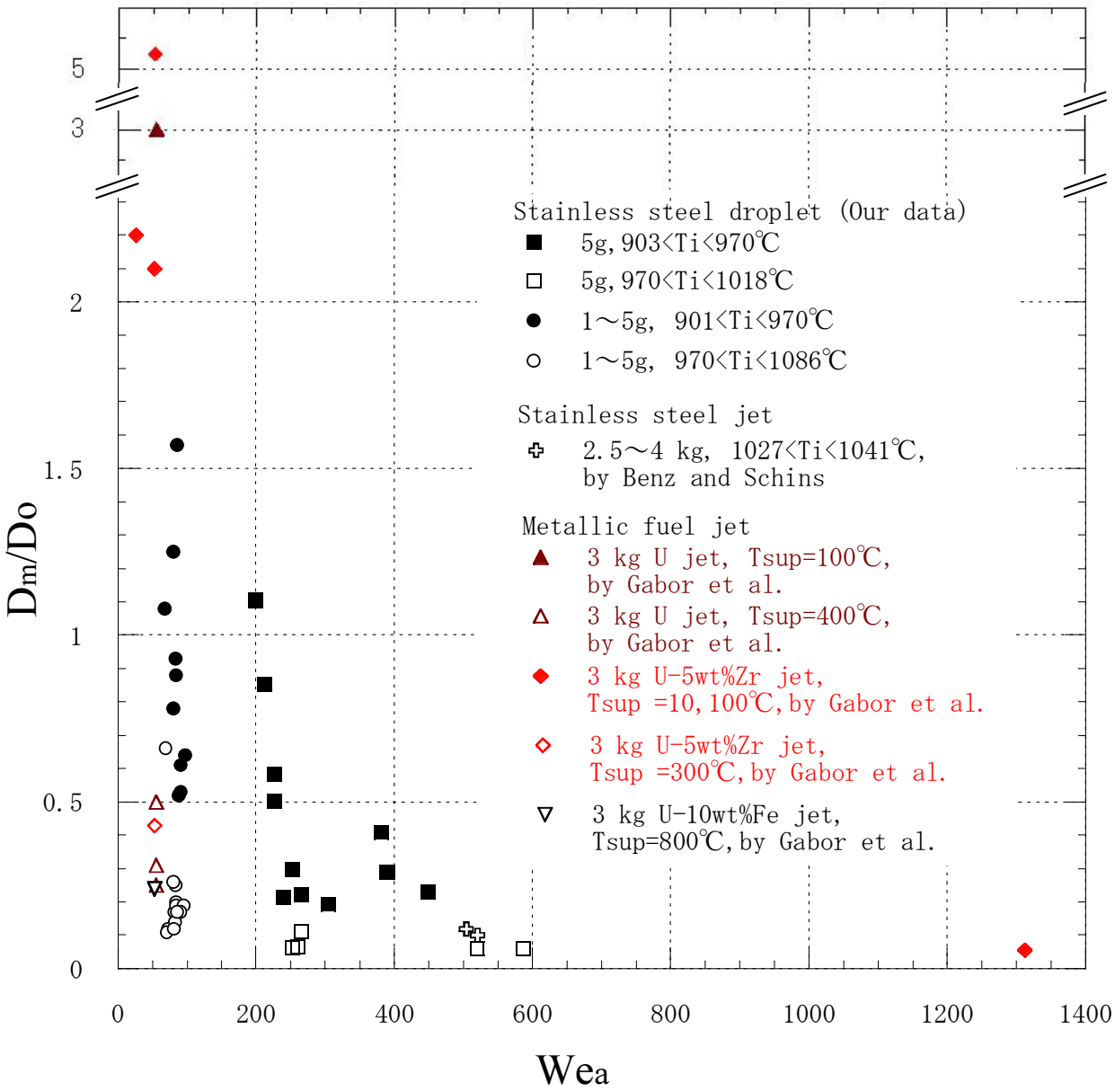

Fig. 6 D_m/D_o versus We_a of 304SS droplet and jet fragments with different T_i

Background (3)

—ULOF image (typical ATWS event) from JAEA

ULOF:Unprotected loss of flow, ATWS:Anticipated transient without scram

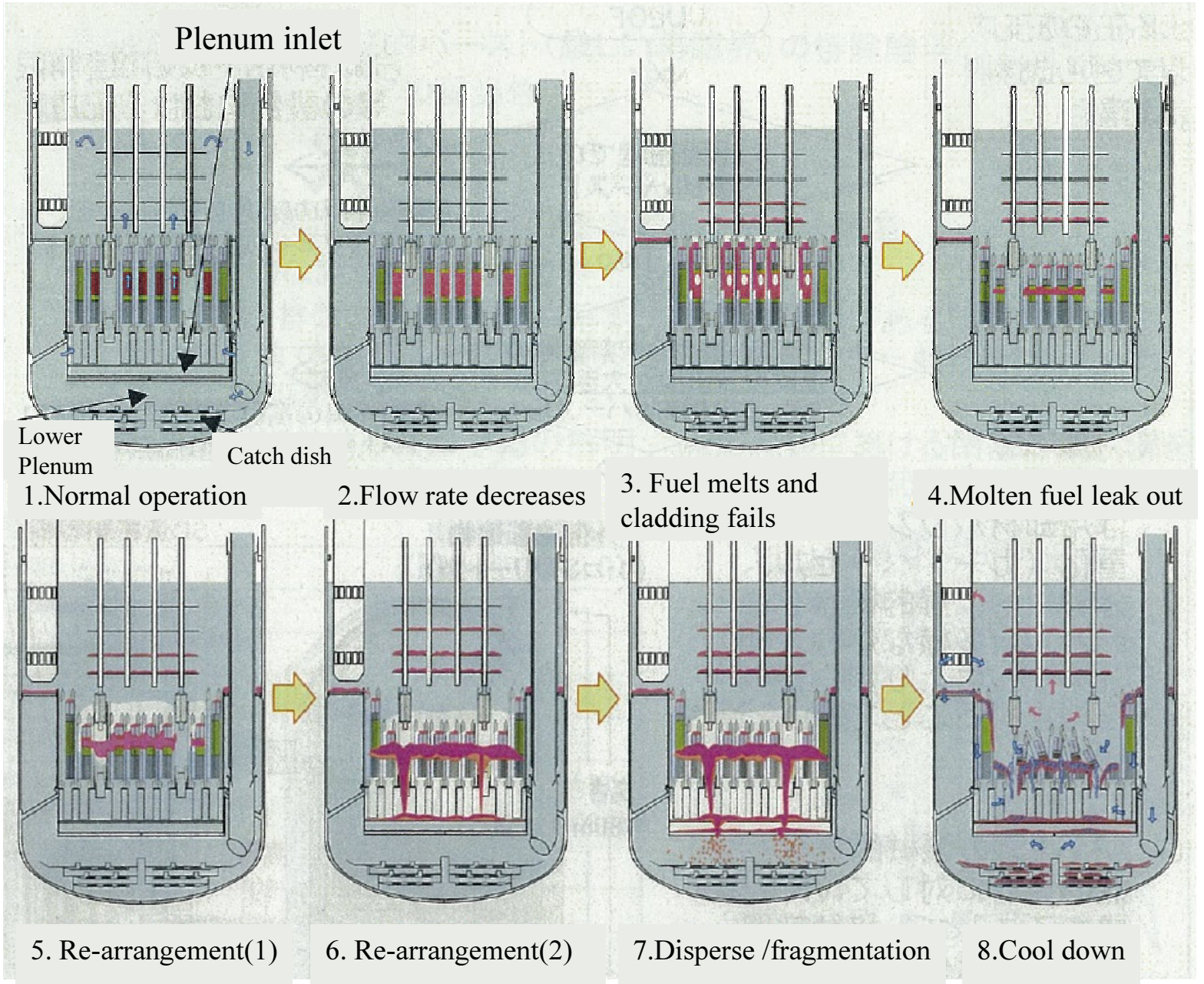

Temperature condition of SCI for molten stainless steel with high We_a and sodium

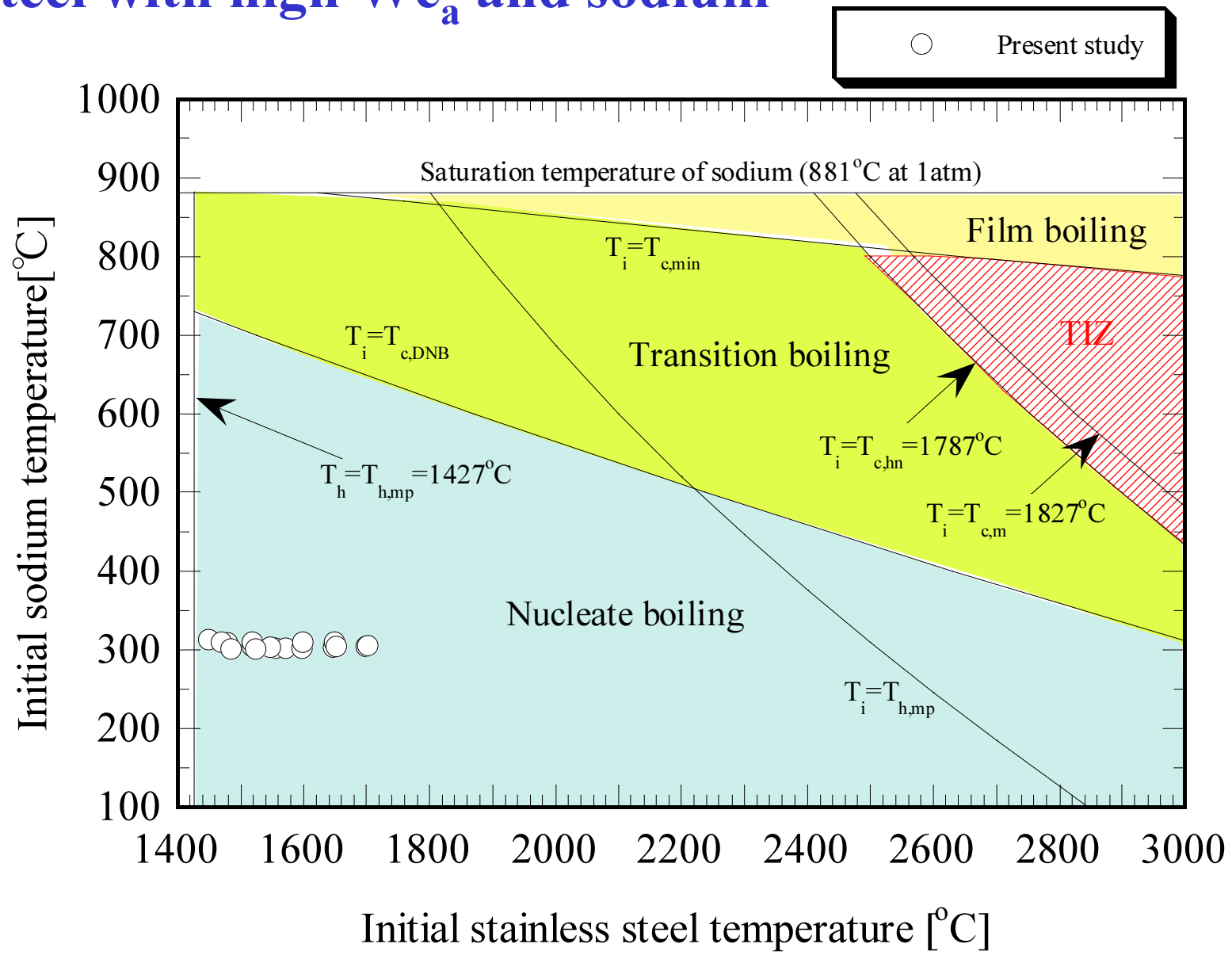

Melting temperature of different metal in Reactor

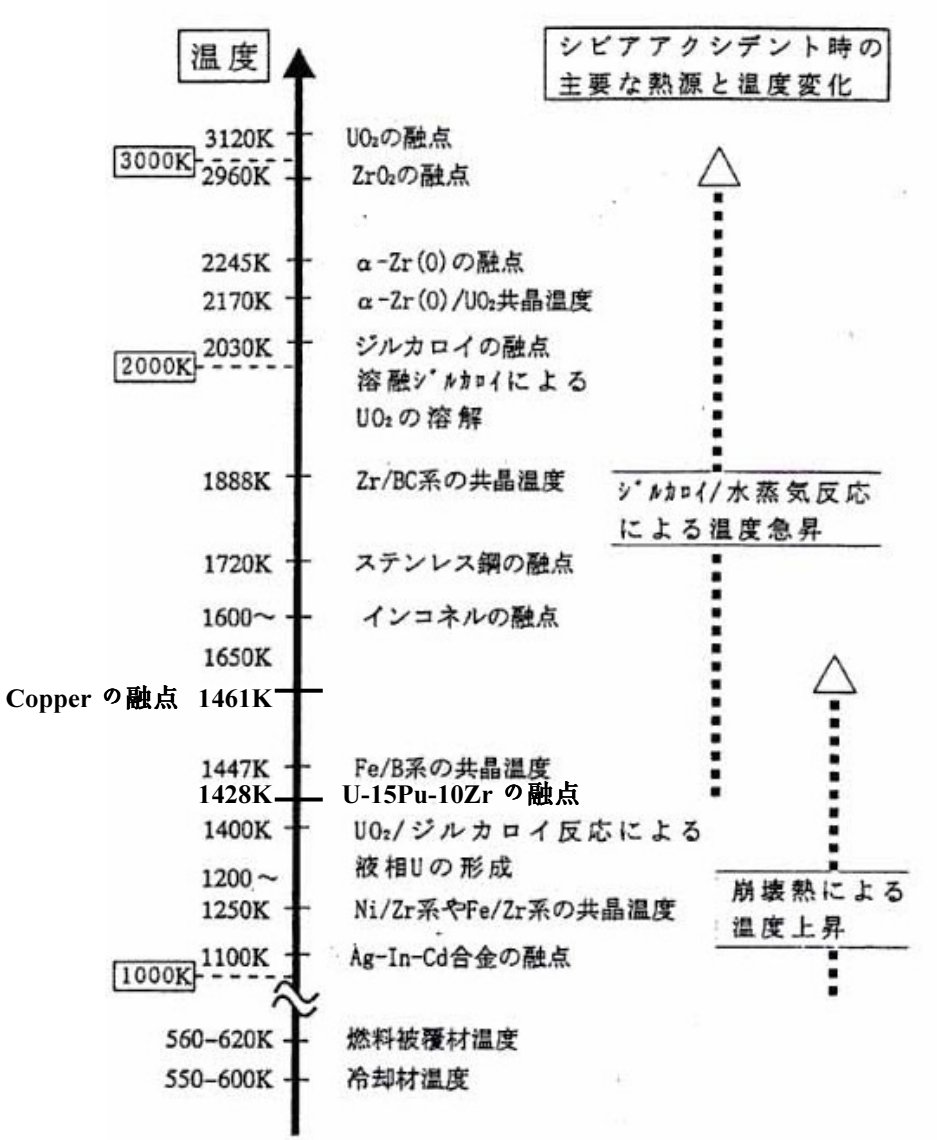

Instantaneous contact interface temperature (T_i)

The temperature is calculated as a one-dimensional heat conduction problem, which does not take the release of latent heat to calculate.

$$T_i = \frac{T_c + T_h \left(\lambda_h \rho_h C_{ph} \Big/ \lambda_c \rho_c C_{pc} \right)^{1/2}}{1 + \left(\lambda_h \rho_h C_{ph} \Big/ \lambda_c \rho_c C_{pc} \right)^{1/2}}$$

T_c: initial temperature of sodium (^oC)
T_h: initial temperature of droplet (^oC)
C_p : specific heat (kJ/kg/ ^{o}C)
λ : thermal conductivity (W/m/ ^{o}C)
ρ : density (kg/m^3)

Subscripts
c : cold liquid
h : hot liquid

Reference:H. S. Carslaw and J. C. Jaeger, *Conduction of Heat in Solids*, 2nd ed., Clarendon Press, Oxford, 282-289 (1959).

Back

Results analysis （5）

Breakup behavior of wood's metal in water with high We_a

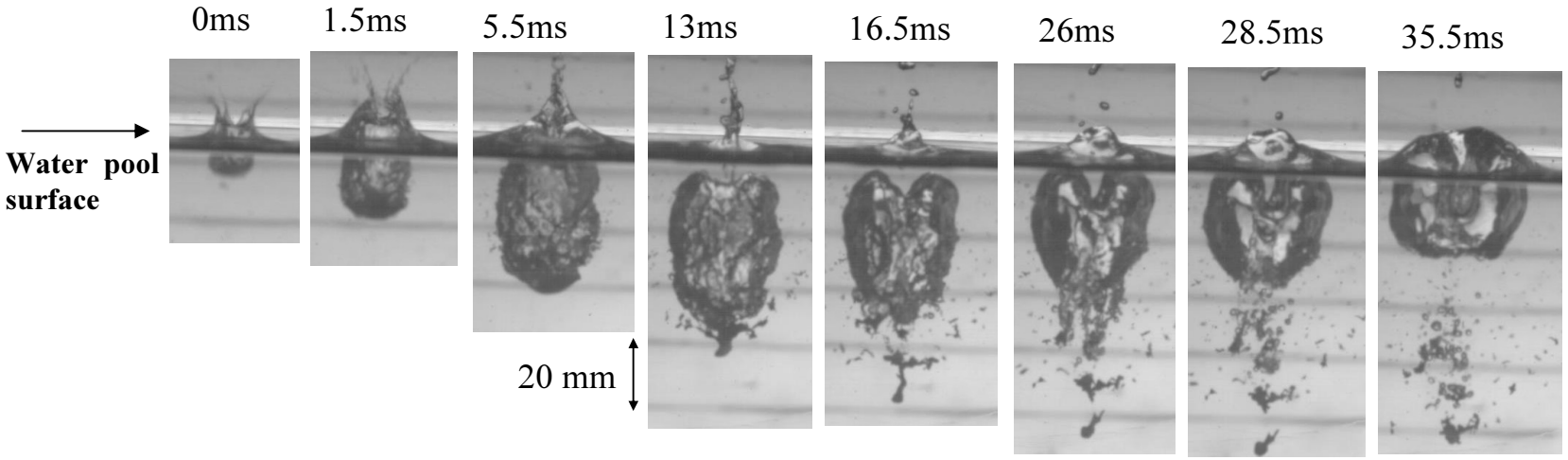

Fig.7 Breakup behavior of wood's metal in water (76℃; 3 g; Water:20℃；We_a:586)

Boundary Layer Stripping Model (Ranger and Nicholls,1969)

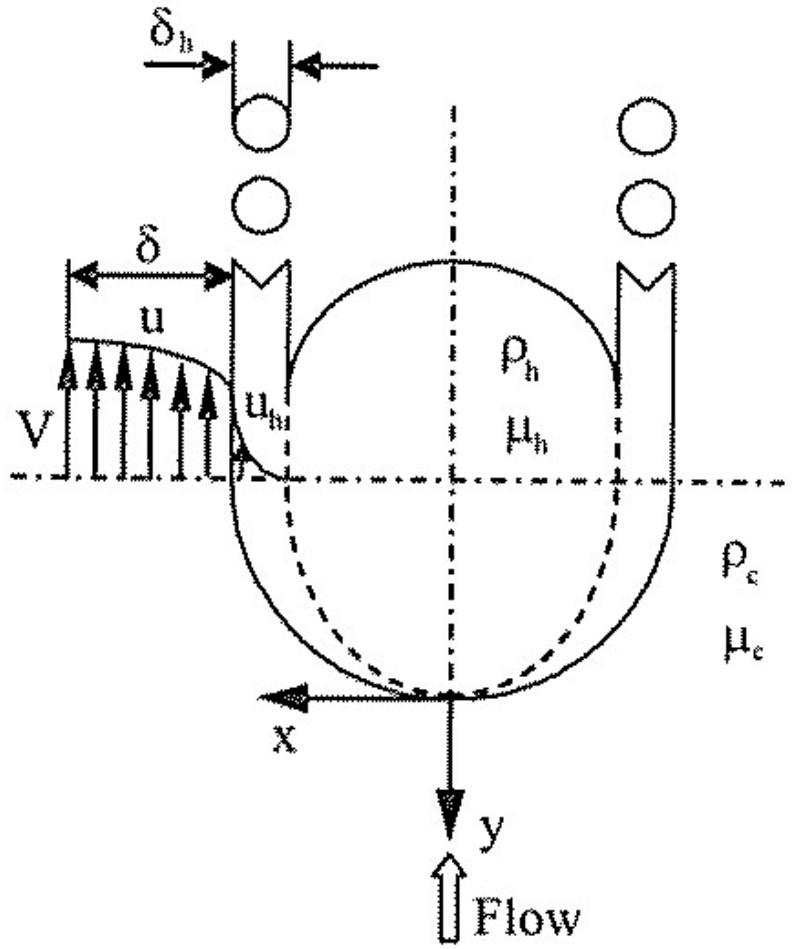

Fragmentation Mechanism of a Molten Metal Jet with Solid Crust

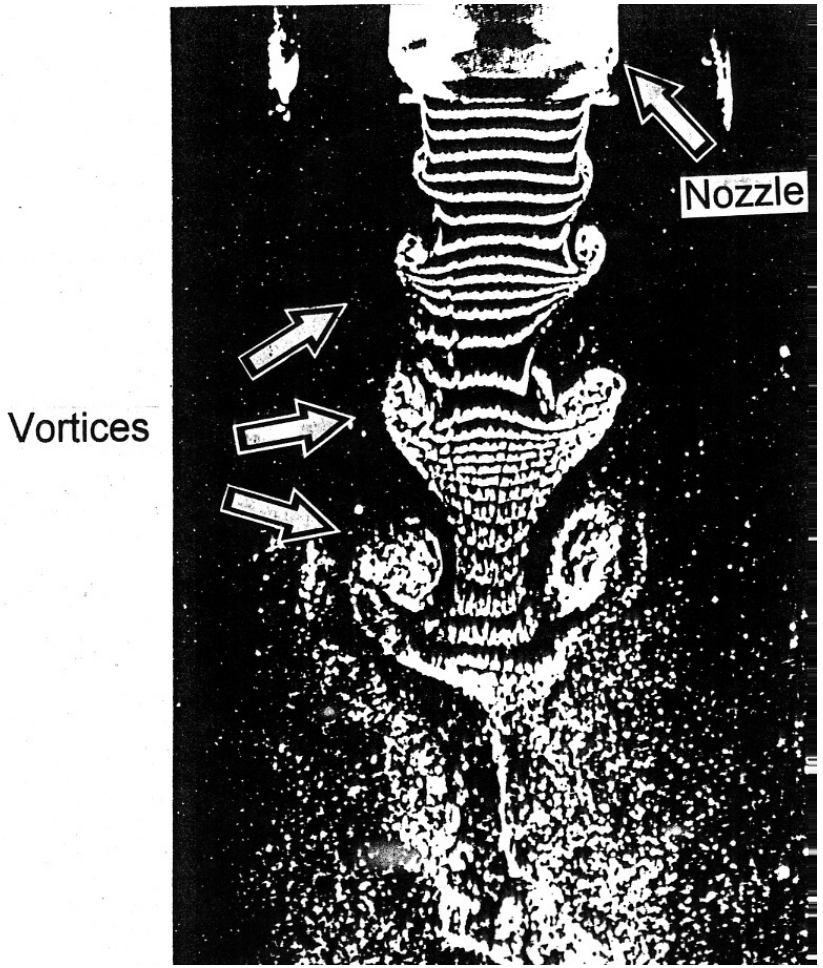

Organized motion between water jet and the surrounding water

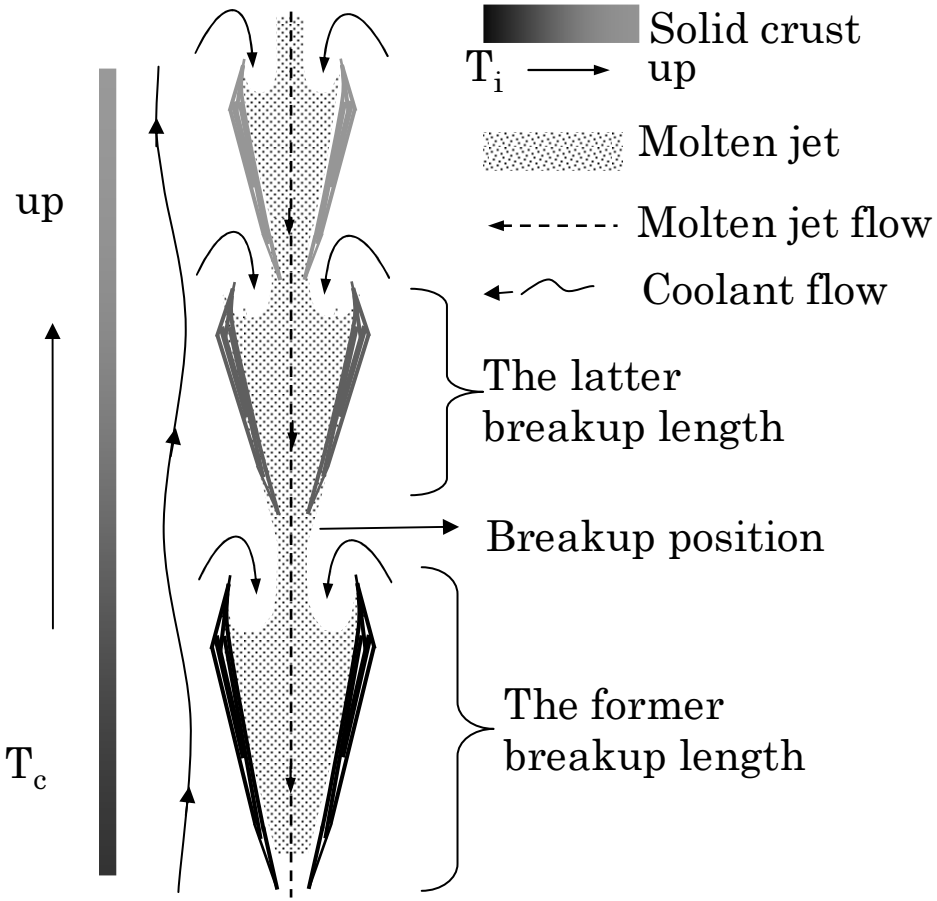

Organized motion between molten Cu jet with solid crust and Na coolant

Previous Experimental Study (1)

Fragmentation of a single molten metal droplet penetrating sodium pool -Comparisons of thermal and hydrodynamic fragmentation-

by Zhang, et al., Presented in *Proc. 17th Int. Conf. on Nucl. Eng. (ICONE17)*, Brussels, Belgium, July 12-16, 2009, ICONE17-75390.

Our group confirmed that the hydrodynamic effect in fragmentation at We_a>200 becomes predominant over the thermal effect under the low superheat condition by conducting a series of experiments of the molten copper droplets (1－5 g) with a wide ambient Weber number (52－614) and superheat temperature penetrating a sodium pool compared with the results of copper jet.

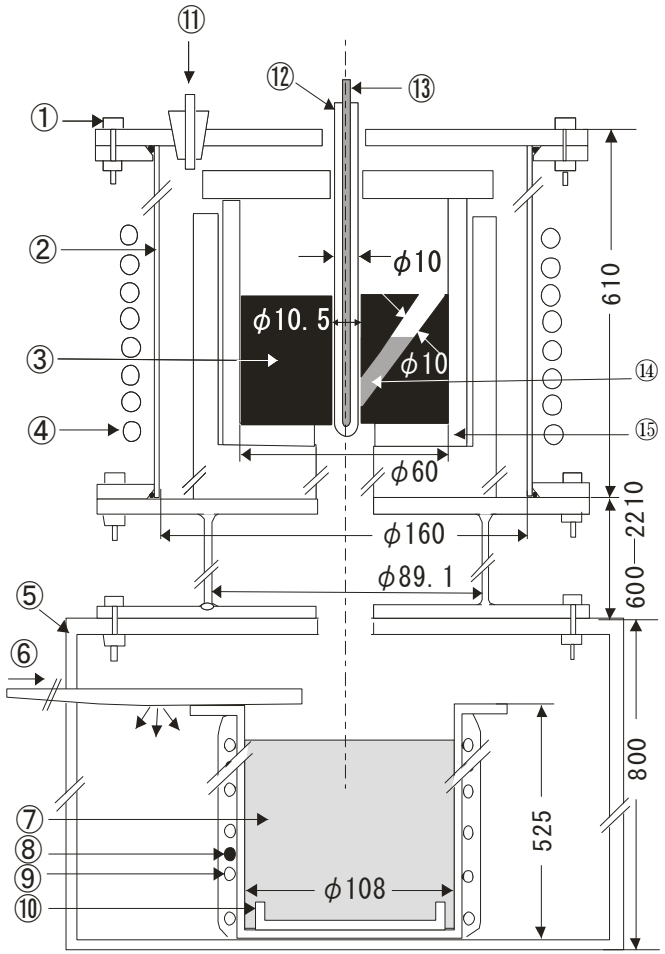

Apparatus for Droplet Breakup

Fragment Size Distribution vs. Mass Median Dia.

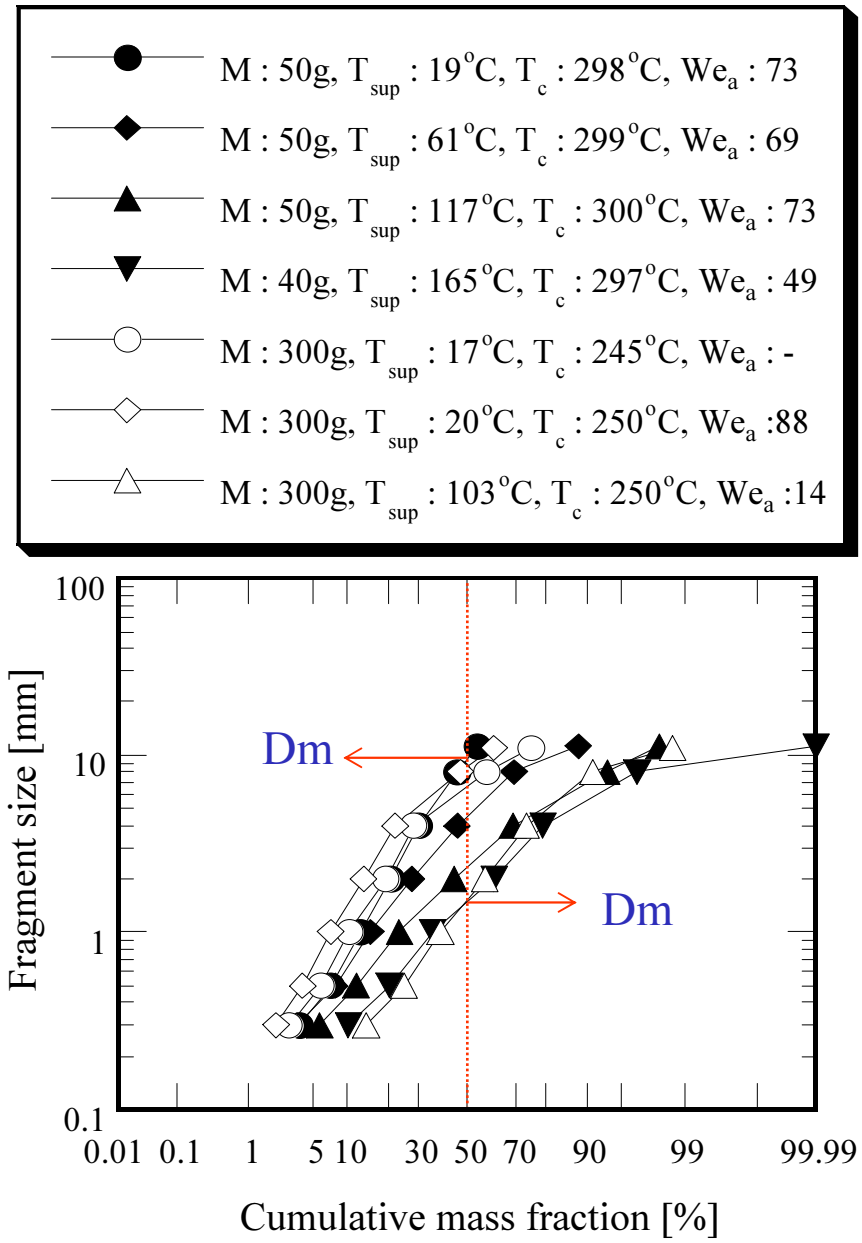

Fragment size distributions of molten Cu jet

Large Fragments with Large-Scale Structure Deformed by Organized Motion

Fragment of Cu jet column with large-scale structure frozen in **sodium** pool
(T_{sup}: 16℃, T_i:1024℃, We:33～42)

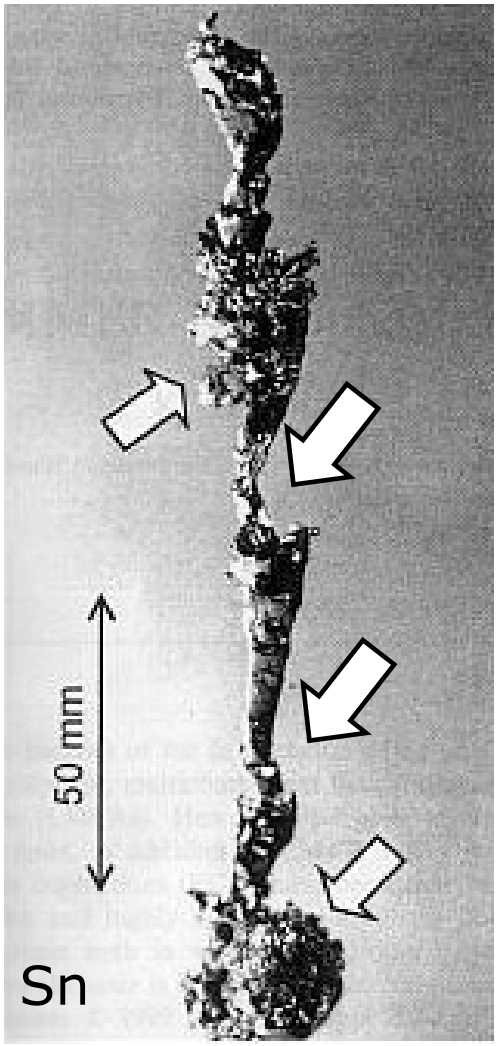

Fragment of Sn jet column with large-scale structure frozen in **water** pool
(T_i<$T_{Sn,mp}$, We:23)